Polymer Drying. X. A Reconsideration of the Kinetics of Evaporation from Polymer–Liquid Systems During the Interval of Transition from the Rubbery to a Glassy State

L. A. ERREDE,* P. J. HENRICH,† and GEORGE V. D. TIERS

3M Corporate Research Laboratories, 3M Center, Bldg. 201-2N-22, St. Paul, Minnesota 55144

SYNOPSIS

This kinetic restudy of the physical changes that occur during evaporation-induced transition from the rubbery to a glassy state of polystyrene–liquid systems shows that such transitions occur via two mechanistic pathways. The first is random nucleation of microdomains of self-associated polymer segments owing to a time-dependent logarithmic decrease in the number of adsorbed volatile molecules per phenyl group of residual mobile polymer segments. The second is a thermodynamically driven self-association of adjacent monomer units with concomitant expulsion of the adsorbed molecules, which appears to propagate via a "domino-like" chain reaction. Conceptually this is a three-dimensional "zippering-up" of suitably close polymer segments to produce the corresponding macrostructural network of self-associated polymer. The kinetics of the latter is zero-order, and this dominates the overall kinetics of evaporation during the latter portion of the transition interval, presumably owing to changes in entropy of the system as it progresses from the mobility characteristic of the rubbery state to the rigidity characteristic of a glassy state. © 1994 John Wiley & Sons, Inc.

INTRODUCTION

Our studies[1] of liquid sorption by poly(styrene-co-divinylbenzene) [hereinafter referred to as poly(Sty-co-DVB) or $(Sty)_{1-x}(DVB)_x$] has shown that the volume ($\mathbf{S}$) of sorbed liquid per gram of polymer at liquid saturation varies linearly with the cube root of the average number (λ) of backbone carbon atoms in the polystyrene segments between crosslink junctions, as expressed by eq 1.

$$\boldsymbol{S} = \boldsymbol{C}(\lambda^{1/3} - \lambda_0^{1/3}) = \boldsymbol{C}\Lambda \qquad (1)$$

Here λ_0 is the value of λ extrapolated to $\boldsymbol{S} = 0$ at 23°C, and the difference $(\lambda^{1/3} - \lambda_0^{1/3})$ is the relative "looseness" (Λ) of the macrostructural architecture of the $(Sty)_{1-x}(DVB)_x$ sample that supports the gel at liquid saturation. The slope ($\boldsymbol{C}$, in mL of *ad*sorbed liquid per gram of polymer) of the linear relationship [eq. (1)] is defined as the "relative swelling power" of the sorbed liquid. We noted[1-4] that $\mathbf{C}$ varies very sensitively with the molecular structure of the sorbed liquid, and that its value is reproducible to ±1 in the third significant figure.

We showed[5] that the Flory–Huggins Interaction Parameter, χ, for polystyrene–liquid (PS–L) systems varies with the corresponding $\boldsymbol{C}$ [eq. (1)], as expressed by eq. (2).

$$\chi_\nu = \mathbf{0.49} + \mathbf{1.01}\nu - \mathbf{0.61}\nu\boldsymbol{C} \qquad (2)$$

Here ν is the volume fraction of polymer in the PS–L system at 23°C. The reproducibility for measuring χ_ν by the usual experimental methods varies with ν, being about ±1 in the second significant figure when ν is equal to 0, and about ±1 in the first significant figure when ν is equal to 1. Equation (2) indicates that χ_ν is most sensitive to the molecular structure of the sorbed liquid when $\nu = 1$, where the usual

* To whom correspondence should be addressed.

† A graduate student in the Department of Chemical Engineering & Materials Science at the University of Minnesota, who has been a part-time employee in our laboratories from 1989 to the present.

Journal of Applied Polymer Science, Vol. 54, 669–696 (1994)
 CCC 0021-8995/94/050669-28

experimental methods for measuring χ_ν are the least reproducible; indeed eq. (2) allows one to calculate χ at $\nu = 1$ within ± 1 in the third significant figure. This permits meaningful correlation of χ_ν with the molecular structure of the sorbed liquid by measurement of its relative swelling power, $\boldsymbol{C}$.

We reported,[1,3] however, that the molecular nature of sorption processes can be interpreted more meaningfully on the basis of the adsorption parameter (α), i.e., the number of *ad*sorbed molecules per accessible phenyl group in the polymer at liquid saturation. The value of α is calculated directly from the corresponding observed $\boldsymbol{C}$ (eq. 1) by means of eq. (3).

$$\alpha = \mathbf{104Cd/M}, \tag{3}$$

where **d** and **M** are, respectively, the density and formula weight of the sorbed liquid, and 104 is the formula weight of a monomeric styrene unit. Substitution of eq. (3) into eq. (1) gives eq. (4), which relates the total number (Σ) of sorbed molecules per phenyl group to α for the liquid and the relative "looseness" [Λ; $\Lambda = (\lambda^{1/3} - \lambda_0^{1/3})$] of the polymer macrostructure.

$$\Sigma = \alpha\Lambda \tag{4}$$

Our sorption studies,[1,3] using homologous series of liquids ZR (in which the functional group Z was kept constant and the rest of the molecule R was varied systematically), showed that α increases with the affinity of Z for the phenyl groups in the $(\mathrm{Sty})_{1-x}(\mathrm{DVB})_x$ sample and decreases with the "bulkiness" of R in accordance with expectation based on simple physical–organic chemical concepts.

Our studies[6–12] of evaporation of PS–L systems from saturation to virtual dryness verified that the sorbed molecules are indeed present in two adsorption states as expressed by eq. (4); namely those that are *ad*sorbed to the polymer (that supports the gel) at liquid-saturation and those that are not so *ad*sorbed. Although the two types are in exchange equilibrium with one another, it is possible to distinguish between them kinetically[6–9] and also spectrometrically.[10–12] The sorbed-but-not-adsorbed molecules are eliminated first, and the kinetics of evaporation with respect to the number (α_t) of residual adsorbed molecules per phenyl group at time t is zero-order, as expressed by eq. (5).

$$\alpha_t = \alpha_0 - rt \tag{5}$$

where α_0 is the number of adsorbed molecules per phenyl group at $t = 0$, and r is the zero-order rate constant in molecules per phenyl group per minute.

When α_t decreases to the composition α' that marks complete elimination of the nonadsorbed molecules, the kinetics of evaporation changes qualitatively from zero-order to first-order, such that α_t is given by a single exponential decay function as expressed by eq. (6).

$$\alpha_t = \alpha' e^{-k't} \tag{6}$$

Here k' is the first-order rate constant (in min^{-1}) for elimination of adsorbed molecules from the PS–L system in its rubbery state, and t is the time after α_t becomes equal to α'.

Deviation from the linearity expressed by the logarithmic form of eq. (6) occurs when α_t becomes equal to α'_g, the composition that marks incipient transition of the PS–L system from its rubbery state to its glassy state, i.e., when the PS–L system begins to undergo evaporation-induced polymer–polymer association such that the mobility of the polystyrene segments in the crosslinked network decreases monotonically from that characteristic of the rubbery state to the rigidity characteristic of the glassy state at α_g. The time interval that the PS–L is undergoing this transition is defined as the transition interval.

Upon completion of this transition (i.e., when α_t becomes equal to α_g), the kinetics of evaporation is given thereafter by a linear combination of **n** (not more than 6) exponential decay functions[6–13], as expressed by eq. (7).

$$\alpha_t = \alpha_g \sum_{i=1}^{n} f_i e^{-k_i t} \tag{7}$$

Here k_i is the first-order rate constant (in min^{-1}) for decay of the ith population, f_i is the fraction of α_g (i.e., α_i/α_g) trapped in the i-th population at the completion of the transition, i is the numerical identification of the population in the sequence of decreasing decay rate k_i, and t is the time after α_t becomes equal to α_g.

We showed[13] that these populations, created during the transition interval, reflect the unique molecular environment in which the "guest molecule" is entrapped. The value of α_g is determined by an iterative mathematical protocol involving sequential subtraction of the logarithmic forms of each of the functions that comprise eq. (7), the iteration beginning with the population having the slowest decay rate and ending with the population having

the fastest decay rate, as described in detail elsewhere.[7-13] When a time study is carried out long enough for at least half of the population with the slowest decay rate to be eliminated, the value of $(\Sigma\alpha_i)/\alpha_g$ is usually 1.00 ± 0.01. This demonstrates that the protocol for isolating each of the functions that comprise eq. (7) does account for virtually all of the trapped molecules present when α_t was equal to α_g.

We reported[8,9] that the compositions α', α'_g, and α_g, identified by the sequential breakpoints in the kinetics of evaporation as described above, vary with the adsorption parameter [α; eq. (4)] of the sorbed liquid as expressed by eqs. (8) to (10).

$$\alpha' = \mathbf{0.33}\Lambda(\alpha + \mathbf{1}) \tag{8}$$

$$\alpha'_g = \mathbf{0.10}\Lambda(\alpha + \mathbf{1}) \tag{9}$$

$$\alpha_g = \mathbf{0.055}(\alpha + \mathbf{1}) \tag{10}$$

We also reported[7-9] that k_1 [eq. (7)] is equal approximately to k' [eq. (6)], and that the logarithms of the set of k_i [eq. (7)] for a given PS–L system in its glassy state decreases incrementally with i in accordance with eq. (11).

$$\mathbf{Log}\ k_i = \mathbf{Log}\ k_0 - mi, \tag{11}$$

Here k_0 and m are constants characteristic of the PS–L system. Our studies of evaporation from PS–L systems as a function of temperature[13] showed that the rate constants k_i depend primarily on entropic effects rather than enthalpic, which is consistent with the point of view that the residual volatile molecules in a glassy state are trapped in different molecular environments that represent polymeric inclusion complexes, from which the difficulty of escape increases incrementally with i by a factor of m, as indicated in eq. (11). The numerical value of i appears to reflect the number of phenyl groups that comprise the "retaining walls" of the "guest"-molecule–"host"-polymer complex.[13]

Although k_i varies with i, as expressed by eq. (11), the fraction (f_i) of the total number of entrapped molecules that comprise a given population at α_g does not vary monotonically with i. The correlations of f_i with i (see Figs. 9 to 11 of ref. 7) usually show maximal f_i-values averaging about 0.25 (but ranging from 0.15 to 0.50) at i = 3 and 4, minimal f_i-values averaging about 0.10 (but ranging from 0.05 to 0.20) at i = 1 and 6, and intermediary f_i-values averaging about 0.16 (but ranging from 0.05 to 0.25) at i = 2 and 5. The large variance in the f_i-data for a given population created during the transition interval of a given PS–L system is presumed to be attributable to lack of control of the various factors that affect the poorly understood mode of self-association as that system goes from its rubbery state to a glassy state.

Because the tangential slope of a Log α_t vs. t plot[7-13] almost always appeared to decrease monotonically with t during the transition interval (i.e., the interval exhibits a concave-upward pattern, as noted in Fig. 21 of ref. 1), it was assumed that the mechanism involves statistically random nucleation of polymer polymer self-association, corresponding to the logarithmic decay of adsorbed molecules [eq. (6)] via evaporation, which is accompanied by progressive growth of the microdomains created thereby. Conceptually this is analogous to crystallization from solution or melt. The polymer transition process, however, appears more complicated than that for the analogous crystallization process, even in those cases for which nucleation and subsequent growth of the microcrystalline domains are both very slow.

Our recent studies of swelling and deswelling of poly(Sty-co-DVB) samples in binary solutions,[14] however, inadvertently provided us with a means for evaluating at least the general validity of the above assumptions. In these studies the volume fraction (z) of the second component in the sorbed binary solution was increased from z = 0 to z = 1 in increments of about 0.1 and then decreased in like manner back to z = 0. The results obtained thereby showed clearly that the history of the poly(Sty-co-DVB) sample affects the sorption capacity of that sample with respect to a given binary liquid composition. Our desorption studies[15] that monitored subsequently the evaporation of the sorbed liquid, before and after the PS–L system had been cycled at saturation from z = 0 to 1 and back to 0, showed that the history of that system in its saturated gel state affects markedly the kinetics of evaporation to virtual dryness, especially after that system begins to undergo evaporation-induced transition from the rubbery state to a glassy state.

Unlike the earlier time studies of evaporation using PS–L systems that had been exposed only to a single test liquid, which usually exhibited Log α_t vs. t patterns during the transition interval that were concave upward, as described above, the corresponding patterns for evaporation from PS–L systems that had been exposed to binary solutions were usually concave downward (see Figs. 2, 3, and 5 of ref. 15), i.e., the tangential slope decreased only during the initial part of the transition interval, but

then *increased* (uncharacteristically) during the rest of that interval, which implies that transition from the rubbery state to a glassy state was occurring *via* an abnormal pathway that enhanced the rate of elimination of the residual sorbed molecules.

We postulated that it might be possible to characterize the kinetics for this "abnormal" pathway by curve-fitting to the sequential subintervals that comprise an "abnormal" transition interval. Comparison of these data with the corresponding data for a "normal" transition interval might afford clues to the mode of polymer–polymer association *via* both types of pathways. The purpose of this publication is to report the results of such kinetic comparisons and the conclusions deduced therefrom.

EXPERIMENTAL

Kinetics of Evaporation During the Transition Interval

The microporous composite film samples, comprised of $(Sty)_{0.98}(DVB)_{0.02}$ particles (80% dry weight) enmeshed in poly(tetrafluoroethylene) [PTFE] microfibers, were prepared as described in detail elsewhere.[2,3] A composite film sample (1.85 g), which had been used in the time studies described in our preceding publication,[15] was "cleaned" by extraction in acetone and then dried to constant weight in a vacuum oven kept at 100°C. The sample was then swelled to saturation in toluene and then deswelled "to saturation" in a binary solution of test liquid that contained less than 0.1% toluene at the end state, as described previously.[14,15] Thereafter the liquid-saturated sample was extracted (every half hour) with fresh test liquid for at least two hours, to ensure removal of all residual non adsorbed toluene, before the start of the time study of evaporation which was carried out under conditions that precluded sample shrinkage as described in the Experimental section of ref. 15. In those cases for which the test liquid was *n*-heptane or methanol, more than two days of extraction in fresh test liquid was needed to remove the last traces of entrapped toluene before the start of the time study of evaporation to dryness, but in those cases for which acetone, chloroform or toluene was the test liquid (i.e., one with good affinity for polystyrene) no more than one extraction for only ten minutes was sufficient for this purpose.

The weight (W_t) of residual sorbed molecules was monitored from liquid saturation to virtual dryness essentially as described in the Experimental section of ref. 8, with the exception that a stainless steel wire mesh was used instead of the aluminum frame (shown in Fig. 1 of ref. 8) to restrain sample shrinkage. The evaporation data obtained thereby were processed by means of the computer program written by Dr. J. W. C. Van Bogart,[7] which enabled us to identify the four successive stages of evaporation, namely (1) the interval for elimination of the nonadsorbed molecules [i.e., from α_0 to α' (eq. (5))], (2) the interval for elimination of adsorbed molecules from the PS–L system in its rubbery state [i.e., from α' to α'_g (eq. (8))] before onset of transition to a glassy state at α'_g [eq. (9)], (3) the interval of evaporation induced transition from the rubbery state to a glassy state [i.e., from α'_g to α_g], and finally (4) the elimination of residual molecules trapped in various populations ($\alpha_{t,i}$) of the PS–L system in its glassy state [eq. (12)], as described previously.[7,8] This involves sequential point-by-point subtraction of the contributions from populations that comprise eq. (12), beginning with the population with the slowest decay rate (represented here by eq. (12, **n**) and ending with that for the fastest (represented here by eq. (12, 1), in which the relationship $\alpha_g f_i$ is equivalent to $\alpha_{t,i}$ at $t = 0$.

$$\mathbf{Log}\ \alpha_{t,n} = \mathbf{Log}(\alpha_g f_n) - (k_n/2.3)t \qquad (12, \mathbf{n})$$

$$\vdots \qquad \vdots \qquad \vdots$$

$$\mathbf{Log}\ \alpha_{t,1} = \mathbf{Log}(\alpha_g f_1) - (k_1/2.3)t \qquad (12, 1)$$

The first data point, in the set of data that comprise the population ($i = 1$) with the fastest decay rate, identifies the composition α_g that marks completion of the transition from the rubbery state to a glassy state.

The modified data set, obtained thereby, was reexamined by the same curve-fitting procedure applied to the original data set, to identify the first two stages of evaporation. These are, namely, from $\alpha_t = \alpha_0$ to $\alpha_t = \alpha'$, which follows zero-order kinetics as expressed by eq. (5), and from $\alpha_t = \alpha'$ to $\alpha_t = \alpha'_g$, which follows first-order kinetics as expressed by eq. (6). The onset of transition from the rubbery state to a glassy state is usually signaled by a decrease in the apparent first-order rate constant. Sometimes, however, it is signaled by a qualitative change in kinetics from first-order to zero-order, which is followed soon thereafter by return to first-order kinetics, the rate constant for which is usually less than that for k'. The end of this subinterval is signaled by deviation from the linearity of first-order kinetics. In cases for which the deviation was negative, i.e., concave upward, the data points following this region were again computer tested for confor-

mity to first-order kinetics. In cases for which the deviation was positive, i.e., concave downward, the data points following this region were computer tested for conformity to zero-order kinetics. The end of this subinterval of zero-order kinetics was in turn signaled by upward concavity. Since this latter deviation could be attributed either to a quantitative change in zero-order rate constant or to a qualitative change in kinetic order from zero to first, the data following thereafter was tested for conformity first to zero-order kinetics and then to first-order kinetics. In this way all of the subintervals that comprised the transition interval, i.e., from α_g' to α_g (the original data set having been modified by the subtractive operation described above), were characterized with respect to kinetic order, rate constant, duration of the subinterval, and the weight loss due to evaporation during that subinterval. These results may be compared to the corresponding curve-fitting results, obtained in like manner, but using the original data set before modification *via* point-by-point subtraction of the contributions from the populations trapped in the glassy state as described above.

Identification of Volatile Species Eliminated During the Transition Interval

Evaporation from a liquid-saturated composite film sample, comprised of $(Sty)_{0.98}(DVB)_{0.02}$ particles enmeshed in PTFE microfibers, was monitored gravimetrically as described above with the modification that the time study was interrupted at predetermined residual weight values (W_t) to permit isolation and subsequent identification of the volatile species being then eliminated. When the value of W_t decreased to the first of the set of predetermined residual weight levels, the sample was placed in a 25 cc vial and sealed by means of a special cap that was fitted with a PTFE septum. After a suitable time interval (which was increased from 5 min to 20 min as W_t decreased from 2.0 to 0.02, to ensure equilibration of the sample with vapor), an aliquot of the vapor-air mix was removed by means of a microsyringe. This gas sample was analyzed by means of a Hewlett-Packard 5890 gas chromatograph fitted with a flame-ionization detector and a 30 meter 5% phenyl silane capillary column, the oven temperature being raised at the rate of 20°C per minute. The molar ratios of the components in the vapor revealed the composition of the molecules being desorbed during the interval that the sample was in the stoppered vial.

Immediately after removal of the vapor sample, the composite film sample was again weighed, and desorption under ambient room conditions was then resumed and continued until the residual weight indicated that the next predetermined weight level had been reached. At this point the time study was again interrupted to establish the corresponding composition of the volatile components, as described above. The compositions established thereby were then correlated with the kinetic pattern for decrease in weight of residual adsorbed materials (recorded previously) to verify the physical state of the PS–L system during the interval that the vapor sample was being accumulated in the headspace of the sealed vial.

RESULTS AND DISCUSSION

Five types of PS–L systems had been used to show that the kinetics of evaporation from saturation to virtual dryness is affected by the history of that system in its liquid-saturated state.[14,15] In two of these studies, the $(Sty)_{1-x}(DVB)_x$ sample was swelled to saturation first in a good solvent, such as toluene, and then deswelled "to saturation" in a very poor solvent, such as *n*-heptane or methanol, which produced appreciable liquid-induced polymer–polymer association before the start of the time study of its evaporation to dryness. In the case of *n*-heptane, the pattern obtained thereby (Fig. 1 of ref. 15) appeared to indicate that most of the polymer that had undergone liquid-induced self-association had also undergone liquid-induced transition from its rubbery state to a glassy state before the start of evaporation to dryness, and during which time the residual fraction (ψ) of polymer still in its rubbery state had undergone evaporation-induced transition to its glassy state. In the case of methanol, the pattern obtained thereby (Fig. 1 in this publication and Fig. 3 of ref. 15) appeared to indicate that most if not all of the polymer that had undergone liquid-induced self-association was still in its rubbery state (ψ = ca. 1) even after all of the nonadsorbed molecules had been eliminated by evaporation.

In those cases for which replacement of toluene by a second solvent (*n*-heptane or methanol) induced polymer–polymer association, the residual material entrapped in the PS–L system in its ultimate glassy state ($\psi = 0$) was mostly toluene. We noted, however, that the toluene fraction (ϕ) of those molecules trapped therein varied with the time (τ) that the PS–L system was postextracted with fresh *n*-heptane or methanol (as the case required) before starting the time study of evaporation. That is, ϕ was about 1 at τ = 15 min, but it decreased mono-

tonically to ϕ = ca. 0.02 at τ = 2 days.[15] In those cases for which solvent replacement did not cause liquid-induced polymer–polymer association (toluene by acetone or chloroform, or chloroform by toluene), the decrease in ϕ owing to replacement of adsorbed molecules from the PS–L system in its gel state, is much faster than it is in its self-associated state.

Correlation of Desorbed Species with Macromolecular Architecture

The degree of abnormality exhibited in the kinetics of evaporation during the transition interval varied with the choice of the test liquid used in the above time studies. The magnitude of abnormality ranged from extremely abnormal to virtually normal in the order methanol > acetone > chloroform > toluene as noted respectively in Figures 3, 5, 7, and 9 of ref. 15. In fact, the transition pattern for toluene exhibited by this sample, which had been exposed temporarily to chloroform, was virtually identical to that of normal patterns usually exhibited by a toluene-saturated sample that had not been exposed temporarily to a different solvent (see Fig. 2 of ref. 13).

We chose to begin our reconsideration of evaporation-during-the-transition-interval with the kinetic data already reported for methanol-saturated samples that had been exposed temporarily to toluene (Fig. 3 of ref. 15), because (1) the patterns exhibited during their respective transition intervals were the most abnormal of the cases already studied, (2) these time studies were replicated four times to evaluate the reproducibility of the observed abnormality, and (3) most if not all of the polymer that had undergone methanol-induced polymer–polymer association was still in its rubbery state at the start of evaporation-induced transition from the rubbery state (ψ = 1) to a glassy state (ψ = 0). It was thus reasonable to expect that this system offered us the best possibility for correlating the mode of transition with ψ, as determined from the kinetics of evaporation during the transition interval.

Before doing so it was necessary to establish whether or not the residual toluene, entrapped earlier during methanol-induced polymer–polymer association, affects subsequently the mode in which the residual fraction of the PS–L still in its rubbery state undergoes evaporation-induced transition to its glassy state. For this purpose we used a freshly prepared PS–L sample that had been saturated in toluene, solvent exchanged by methanol, the volume of which was such that it contained less than 0.1% toluene at the end state, and then extracted with fresh methanol every half hour over the next 5 hours before starting the time study of evaporation to dryness.

This time study, however, was interrupted at predetermined weight values (W_t), to identify volatile species, as described in the Experimental section. This permitted correlation of the composition determined thereby with the changes in the macrostructure of the PS–L system that are known to occur sequentially as the system is evaporated to dryness.[11-13] These sequential changes had already been established for polystyrene–methanol systems via noninterrupted time studies that monitored W_t (or the corresponding α_t derived therefrom) from saturation to virtual dryness.[15]

The mole fraction (ϕ) of toluene in the set of 11 samples (A to K) of desorbed gases are recorded in Table I, along with the initial (W_i) and final (W_f) weights of the samples during the respective intervals of interruption. The kinetic patterns for evaporation (between interruption intervals) paralleled the patterns exhibited in Figure 3 of ref. 15. From this it was possible to use W_i and W_f, observed for each of the intervals of interruption, as sequential "benchmarks" that indicated the progressive change in physical state of the PS–L system. The registry of samples A to K (Table I) with the evaporation pattern recorded for Run #3 in Figure 3 of ref. 15 is given in Figure 1.

The measured values of ϕ (Table I) show that during the interval in which sorbed-but-not-adsorbed molecules were being eliminated from the PS–L system in its gel-state (i.e., ψ = 1, in the presence of nonadsorbed methanol molecules), ϕ was less than 0.0001 (sample A), whereas during the intervals in which adsorbed molecules were being eliminated from the system in its rubbery state (ψ = 1, but in the absence of nonadsorbed methanol molecules), ϕ was about 0.01 (samples B, C, and D). This marked difference in ϕ is attributed to adsorption partitioning that favors toluene over methanol, as might be expected from the corresponding marked difference in their relative adsorption parameters (α) with respect to poly(styrene), i.e., 1.99 and < 0.06 respectively.

The ϕ-values for the gas samples E to H (Table I), taken during the interval that the PS–L system was undergoing transition from the rubbery state (ψ = 1) to the glassy state (ψ = 0), are much smaller than those for samples B to D, which were collected during the preceding interval. This seemingly anomalous result would have been difficult to rationalize, if it were not for the visual observations made during the intervals that these samples were being accumulated in the headspace of the stoppered glass

Table I Correlation of ϕ with ψ for Evaporation of Methanol from a PS-L System that had been Exposed Temporarily to Toluene

Sample[a]	W_i to W_f[b]	W_{meth}/W_{tol}[c]	ϕ[d]	ψ[e]	State[f]
A	2.0–1.4	> 30,000[g]	< 0.0001	1	Gel
B	0.63–0.62	42.4	0.008	1	Rubbery
C	0.32–0.30	20.6	0.017	1	Rubbery
D	0.16–0.15	37.5	0.009	1	Rubbery
E	0.08–0.07	105	0.003	> 0.7	Transition
F	0.06–0.05	167	0.002	0.5 to 0.7	Transition
G	0.03–0.02	138	0.003	0.2 to 0.5	Transition
H	0.018–0.014	108	0.003	< 0.2	Transition
I	0.0104[h]	0.430	0.45	0	Glassy
J	0.00574[h]	0.201	0.63	0	Glassy
K	0.0056[h]	0.165	0.68	0	Glassy

[a] Sample sequence in which the gas sample was removed for analysis, as indicated in Fig. 1.
[b] W_i and W_f are the initial and final residual weights for the sampling interval.
[c] W_{meth}/W_{tol} is the weight ratio of methanol to toluene in the headspace in equilibrium with the PS-L sample, which was determined as described in the Experimental.
[d] ϕ-Toluene mole-fraction the gas sample; calculated from W_{meth}/W_{tol}.
[e] ψ the fraction of the PS-L system still in its rubbery state.
[f] The physical state of the PS-L system during the time interval that the desorbed molecules were being accumulated in the headspace.
[g] W_{meth}/W_{tol} determined by J. N. Schroepfer[15] before the start of the time study.
[h] Sample heated to 100°C for 10 minutes.

vials. In the cases of samples E to H, liquid condensation in the form of microdroplets began to accumulate on the inner glass surface immediately after the vial was stoppered, such that about a minute thereafter it was almost impossible to see the sample contained therein. These observations are interpreted to mean that soon after the PS–L system began its transition to the glassy state, a process for

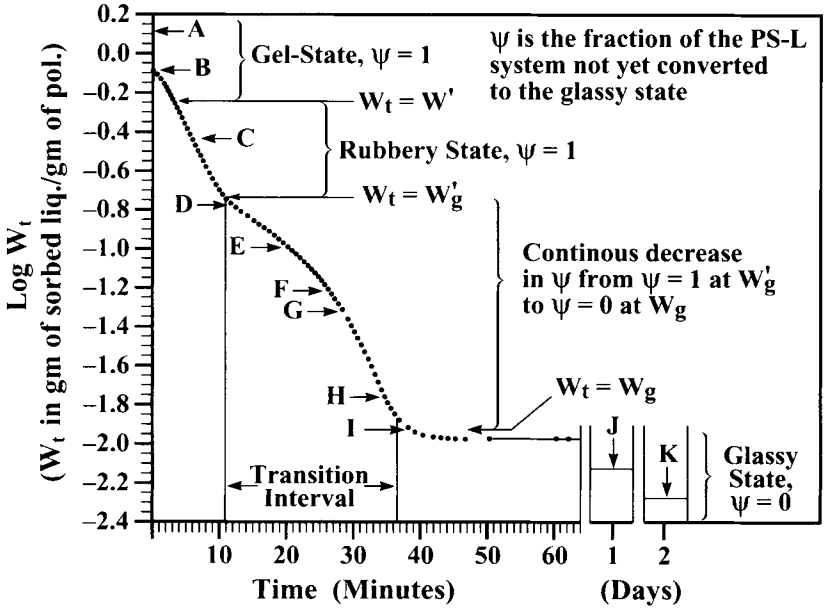

Figure 1 Correlation of gas samples (A through K) with the pattern of evaporation from a methanol-saturated PS–L system that had been swelled to saturation in toluene and then solvent exchanged by methanol. The analysis data for the gas samples are collected in Table I.

polymer–polymer association with concomitant expulsion of adsorbed molecules was initiated. That process could not be arrested even when the partial pressure of methanol in the closed glass vial had attained saturation. This observation is in marked contrast to the complete absence of such condensations in the earlier stages of drying, despite that the PS–L system contained considerably more sorbed volatile molecules.

It follows, therefore, that the gas compositions in the stoppered vials of samples E to H (Table I), were in equilibrium with the condensed liquid rather than metastably with the residual molecules trapped in the polymer. This in effect represents a one-plate distillation; in the case of toluene–methanol mixtures, a threefold enrichment of toluene in the liquid phase is expected. This partition could account for the observed three-fold difference in ϕ-values for samples B to D relative to those for samples E to H. An alternative explanation for the lower ϕ-values is that it may reflect the difference in retentivity of methanol and toluene the system undergoing transition to the glassy state.

When the above PS–L systems are evaporated down to the composition (α_g; eqs 7 and 10) that marks completion of the transition to the glassy state, the rate of desorption decreases dramatically, as noted in Figure 1. Consequently the sample, enclosed in the stoppered glass vial, had to be heated to 100°C for about 10 minutes, to accumulate enough desorbed molecules in the headspace to exceed the minimum requirement needed for gas-chromatographic analysis, in order to determine the ϕ-values recorded for samples I, J, and K (Table I). These data show that ϕ for the residual molecules of the PS–L system in its glassy state is about sixty-fold greater than the corresponding values in its rubbery state (samples B, C, and D; Table I). This enormous difference in ϕ reflects the adsorption partitioning of the components between the binary solution and the sorbent polymer at the moment of capture by liquid-induced polymer–polymer association and before the start of evaporation. The observed ϕ for residual molecules in the glassy state is a lower-limit value for the composition of entrapped species that were present at $\tau = 0$, since ϕ decreases with the time τ that the PS–L system is extracted with methanol before the start of the time-study, which in this case was $\tau = 5$ h.

We repeated this study using a composite film sample that had the same history as that of the former PS–L sample except that it had been extracted with fresh methanol for five days instead of just five hours. This favored the removal of all the toluene that had been entrapped by liquid-induced polymer–polymer association before the start of the time-study of evaporation to dryness. Again condensation on the inner surfaces of the closed system occurred during the interval of evaporation-induced transition, but not during the preceding or subsequent short intervals during which the time study was interrupted for gas sample analysis. Only trace amounts of toluene were present in the gas samples, even in those collected after the PS–L system had attained the rigidity of the glassy state. These results confirmed that the expulsion of adsorbed methanol via the alternate pathway (i.e., the one that is not arrested even when the methanol vapor in the air space above the sample is at saturation) is characteristic of polystyrene–methanol systems and is independent of any residual toluene entrapped earlier during liquid-induced polymer–polymer association.

In view of the above results, we considered it necessary to reexamine our earlier observations,[11,12] namely that desorption from PS–L systems that contain sorbed acetone, chloroform or toluene can indeed be arrested even during the transition interval by placing the sample in a stoppered glass vial. No condensation of desorbed molecules was observed, and on removal each sample weighed virtually the same after three weeks of storage at room temperature in the closed system as it had at the time it was placed therein. These results verify that sorption is reversible, even during the transition interval, when the sorbate molecules have good affinity ($\alpha > 0.6$) for sorbent polystyrene. Irreversibility occurs when the sorbate molecules have poor affinity ($\alpha < 0.06$) for sorbent polymer in the glassy state, such as in the case of methanol.

In retrospect, the above observations follow logically from the respective adsorption patterns (Figs. 7, 11, and 12 of ref. 14), which show marked hystereses with regard to affinity of the liquid for polystyrene before and after temporary exposure to toluene. The affinity of methanol for polystyrene in its glassy state is $\alpha = < 0.06$, whereas for such PS–L systems in the rubbery state it is $\alpha = 0.35$ (Fig. 7 of ref. 14). Thus, methanol molecules expelled during the transition interval are not reabsorbed even when the partial pressure of methanol attains the saturation level, and consequently condensation occurs on the inner surfaces of the closed system as noted above. In the cases of sorbed liquids with good affinity for polystyrene, however, the sorption process is quite reversible because the ratio of the respective α-values before and after exposure to toluene is much closer to unity, and consequently further loss of sorbed molecules is arrested simply by placing

the sample in a closed container, even when that system had undergone complete transition to the glassy state.

On the basis of these results it was concluded that the abnormal kinetics of evaporation during the transition interval is not attributable to residual entrapped toluene molecules, but rather it is characteristic for methanol–polystyrene systems. The normal pathway, which involves continuous elimination of adsorbed molecules from the PS–L system in its rubbery state [as expressed by eq. (6)] that eventually causes polymer–polymer association to occur statistically and randomly throughout the bulk of the system, can of course proceed concurrently with the alternate pathway, despite that elimination of adsorbed molecules via the alternative pathway may dominate the kinetics of evaporation during the second half of the transition interval. These observations support the point of view, stated in the Introduction, that it would be possible to elucidate the manner in which the PS–L system undergoes transition from its rubbery state ($\psi = 1$) to its glassy state ($\psi = 0$) by a more detailed reconsideration of the kinetics of evaporation during this transition. The results observed in regard to this part of our investigation is discussed in the following subsection.

Transition of Methanol Systems from the Rubbery State to the Glassy State

The computerized curve fitting, used earlier to identify the interval for elimination of nonadsorbed molecules and then to identify the interval for elimination of adsorbed molecules before onset of the evaporation-induced transition to the glassy state, was applied to the entire transition interval, as described in the Experimental section. The results obtained thereby for the sequential subintervals that comprise the transition interval are collected in Table II. Each of the subintervals established for the four time studies of methanol evaporation recorded in Figure 3 of ref. 15 are characterized in Table II by (1) the kinetic order exhibited during the subinterval (either zero-order, identified by the number 0, or first-order, identified by the number 1), (2) the numerical value for the 0-th-order ($\mathbf{r}$ in grams of residual sorbed liquid per gram of polymer) or first-order (k, in min^{-1}) rate constants, (3) the initial (P_i) and final (P_f) data points of the interval, (4) the corresponding initial (t_i) and final (t_f) times in minutes after the start of the time study, and (5) the corresponding initial (W_i) and final (W_f) residual weights of sorbed molecules in grams per gram of polymer. The square of the correlation coefficient (R^2) for the straight line of best fit through the subintervals of zero or first-order kinetics was in every case greater than 0.99, and the number of data points that comprised the subinterval was in every case greater than 6 and usually greater than 12.

It is seen in Table II that none of the data points recorded in each of the four time studies are omitted in the corresponding reconsideration by the curve-fitting procedure. These data also show that, in three of the four time-studies of methanol evaporation, onset of the transition interval was signaled by a significant sudden decrease in the first-order rate constant, presumably owing to a collapse of the macromolecular architecture resulting from evaporation-induced polymer–polymer association, which was followed by a long interval of zero-order kinetics. In all four cases this interval of zero-order kinetics was followed by a period of first-order kinetics, just before the PS–L fully attained the rigidity characteristic of the glassy state.

Computerized application to subsequent data points of the iterative subtractive operation used to identify the populations trapped in the glassy state (as described in the Experimental section) confirmed that the final subinterval of the transition interval (noted in Table II) was truly not part of the previously reported linear combination of exponential decay functions [eq. (7)] that characterize the glassy state, despite that the curve fitting to the Table II data set (i.e., before correction for contributions from the glassy state) indicated first-order kinetics for the evaporation during this final subinterval. We concluded from these observations that the major part of the volatile material being eliminated from the PS–L system during the first third of the transition interval is being contributed primarily by the fraction (ψ) of the system still in its rubbery state, as expressed by eq. (6), whereas those being eliminated during the last third of the transition interval are being contributed primarily by the fraction ($1 - \psi$) of the system that had been converted to the glassy state, as expressed by eq. (7).

It was reasoned, therefore, that a more complete understanding of the mode for conversion to the glassy state during the latter portion of the transition interval (i.e., as ψ approaches 0) would have been obtained, if the computerized curve-fitting procedure had been applied after the original data set had been corrected by the computerized operation for sequential point-by-point subtraction of the exponential decay functions represented by eq. (7). This mathematical operation would have reduced or eliminated the complications owing to contributions

Table II Desorption from Methanol-Saturated $(Sty)_{1-x}(DVB)_x$ (*before* "corrections" due to vitrification)

Run[a]	State[b]	Kinetics		Data Points[e] P_i to P_f	Time Interval[f] t_i to t_f	Weights[g] W_i to W_f	R^2 [h]
		Order[c]	Constant[d]				
1	Gel	0	(0.0713)	1–31	0.0–7.5	1.222–0.692	0.9994
	Rubbery	1	0.1004	31–43	7.5–10.5	0.692–0.513	0.9993
	Transition	0	(0.0518)	44–55	10.8–14.0	0.498–0.330	0.9992
		1	0.1456	56–76	14.3–19.3	0.318–0.155	0.9998
		1	0.1220	77–93	19.5–23.5	0.150–0.092	1.0000
		0	(0.0104)	94–106	23.8–27.0	0.089–0.055	0.9995
		1	0.2017	107–114	27.5–31.0	0.050–0.025	0.9997
2	Gel	0	(0.0620)	1–25	0.0–8.0	0.858–0.373	0.9991
	Rubbery	1	0.1452	25–40	8.0–13.0	0.373–0.175	0.9998
	Transition	1	0.1042	40–69	13.0–22.7	0.175–0.065	0.9994
		0	(0.00771)	70–77	23.0–25.5	0.062–0.042	0.9985
		1	0.1873	78–85	26.0–29.5	0.039–0.020	0.9992
3	Gel	0	0.0847	1–16	0.0–5.0	0.830–0.413	0.9976
	Rubbery	1	0.1287	17–31	5.3–11.0	0.390–0.186	0.9932
	Transition	1	0.0608	32–46	12.0–20.0	0.170–0.103	0.9978
		0	(0.00652)	46–66	20.0–30.0	0.103–0.038	0.9990
		0	(0.00476)	67–73	30.5–33.5	0.035–0.021	0.9973
		1	0.1307	73–79	33.5–36.5	0.021–0.013	0.9963
4	Gel	0	(0.0762)	1–16	0.0–5.0	0.791–0.414	0.9978
	Rubbery	1	0.1381	16–29	5.0–11.0	0.414–0.186	0.9928
	Transition	1	0.0622	30–46	12.0–22.0	0.167–0.089	0.9996
		0	(0.00568)	46–62	22.0–30.0	0.089–0.044	0.9990
		0	(0.00434)	62–71	30.0–34.5	0.044–0.024	0.9981
		1	0.1540	71–78	34.5–38.0	0.024–0.011	0.9998

[a] Run refers to the Run No. as designated in Fig. 3 of ref. 15.

[b] State refers to the physical state of the PS-L system. "Gel" is the state in which there are sorbed-but-not-adsorbed molecules as wel as *ad*sorbed molecules as indicated in eq. (4). Rubbery is the rubbery state of the system before onset of the transition interval. Transition is the time-interval during which the system is undergoing transition from the rubbery to the glassy state.

[c] Order refers to the kinetic order of the interval identified. The number 0 indicates zeroth-order (r in grams of sorbed molecules per gram of polymer). The number 1 indicates first-order (k in reciprocal minutes).

[d] Constant refers to the value for the corresponding rate constant (r or k). The values for r are placed in brackets to stress that these are zero-order constants.

[e] P_i and P_f refer, respectively, to the initial and final points of the subinterval.

[f] t_i and t_f refer, respectively, to the initial and final time-values of the subinterval.

[g] W_i and W_f refer, respectively, to the initial and final weights of the subinterval.

[h] R^2 refers to the square of the correlation coefficient of the straight line relationship established for the subinterval, i.e., the "goodness" of the fit.

to the kinetics of evaporation that are derived from the fraction $(1 - \psi)$ of the PS–L system that had been converted to the glassy state during the final third of the transition interval.

Accordingly, the curve-fitting procedure was repeated using the original data set but "corrected" as described above, and the results obtained thereby are collected in Table III, which also records the data for decay of each of the populations trapped in the glassy state, starting with the population ($\boldsymbol{i} = \boldsymbol{n}$) having the slowest decay rate and ending with that ($\boldsymbol{i} = 1$) having the fastest decay rate as described in the Experimental section. The first data point that marks the start of elimination from population $\boldsymbol{i} = 1$ also marks the composition at the end of the transition interval, i.e., α_g.

Comparison of the "corrected" curve-fitting data collected in Table III with the "raw" data for the corresponding subintervals collected in Table II shows that small quantitative differences do exist in these two sets of subinterval data, but they do not show any qualitative change in the kinetic order except for the last subinterval of the transition interval, during which time ψ is close to zero. When

Table III Desorption from Methanol-Saturated $(Sty)_{1-x}(DVB)_x$ (*after* "corrections" due to vitrification)

Run[a]	State[b]	Kinetics		Data Points[e]	Time[f]	Weight[g]	
		Order[c]	Constant[d]	P_i to P_f	t_i to t_f	W_i to W_f	$R^{2\,h}$
1	Gel	0	(0.0713)	1–31	0.0–7.5	1.222–0.692	0.9994
	Rubbery	1	0.1021	31–43	7.5–10.5	0.692–0.513	0.9992
	Trans.	0	(0.0500)	44–59	10.8–15.0	0.498–0.286	0.9986
		1	0.1417	60–102	15.3–26.0	0.275–0.0650	0.9992
		0	(0.00917)	103–110	26.3–29.0	0.0626–0.0374	0.9992
		0	(0.00588)	111–114	29.5–31.0	0.0339–0.0251	0.9959
	Glassy	1	0.2120	114–134	31.0–45.0	0.0251–0.0104	0.9973
		1	0.0666	135–139	50.0–70.0	0.0099–0.0097	0.9906
		1	0.00396	140–143	80.0–260	0.00966–0.00955	0.9824
		1	0.0_4200	144–147	390–1530	0.00945–0.00923	1.000
2	Gel	0	(0.0620)	1–25	0.0–8.0	0.858–0.393	0.9991
	Rubbery	1	0.1508	25–40	8.0–13.0	0.373–0.182	0.9997
	Trans.	1	0.1136	40–67	13.0–22.0	0.182–0.0700	0.9995
		0	(0.00760)	67–80	22.0–27.0	0.0700–0.0321	0.9983
		0	(0.00480)	81–84	27.5–29.0	0.0294–0.0221	0.9915
	Glassy[i]	1	0.1961	85–98	29.5–40.0	0.0203–0.0106	0.9975
		0	(0.0_3215)	99–103	41.0–45.0	0.0103–0.00939	0.9834
		1	0.0542	104–107	55.0–85.0	0.00927–0.00918	0.9783
		1	0.00564	108–111	146–360	0.00913–0.00905	0.9260
		1	0.0_4268	112–114	420–500	0.00902–0.00900	0.9456
3	Gel	0	(0.0847)	1–16	0.0–5.0	0.830–0.413	0.9976
	Rubbery	1	0.1342	17–31	5.3–11.0	0.390–0.186	0.9937
	Trans.	1	0.0673	32–48	12.0–21.0	0.170–0.0957	0.9978
		0	(0.00638)	49–67	21.5–30.5	0.0922–0.0349	0.9990
		0	(0.00476)	67–73	30.5–33.5	0.0349–0.0206	0.9973
		0	(0.00210)	74–79	34.0–36.5	0.0189–0.0136	0.9887
	Glassy	1	0.6251	80–86	37.0–43.0	0.0138–0.01083	0.9963
		1	0.00120	87–98	44.0–1888	0.01079–0.00960	0.9989
		1	0.0_4209	99–102	3089–6247	0.00929–0.00875	0.9897
4	Gel	0	(0.0762)	1–16	0.0–5.0	0.791–0.414	0.9978
	Rubbery	1	0.1420	16–29	5.0–11.0	0.414–0.186	0.9931
	Trans.	1	0.0676	29–46	11.0–22.0	0.186–0.0891	0.9980
		0	(0.00568)	46–62	22.0–30.0	0.0891–0.0436	0.9990
		0	(0.00426)	62–72	30.0–35.0	0.0436–0.0224	0.9973
		0	(0.00264)	73–78	35.5–38.0	0.0207–0.0141	0.9948
	Glassy	1	0.1907	79–94	40.0–55.0	0.0107–0.00762	0.9951
		1	0.00195	95–103	56.0–1485	0.00756–0.00658	0.9891
		1	0.0_4104	104–106	2677–5722	0.00650–0.00625	1.000

Footnotes (a) through (h) are the same as reported in Table II.

[i] Indicates an abnormal subinterval of zero-order kinetics that is observed occasionally during evaporation from the glassy state. When it does occur, it usually does so just before complete elimination of a population ($i = n - 1$) having rate constant k_{n-1} and the start of the elimination of the population ($i = n$) having the next slower decay rate constant k_n, as noted in this example and as discussed in the last section of the text.

curve-fitting was applied to the original data set, the kinetics for elimination of residual adsorbed molecules during the last subinterval (Table II) appeared to be first-order, because (a) virtually all of the PS–L system is in its glassy state [i.e., $(1 - \psi)$ is close to 1], and (b) the kinetics of desorption from the glassy state follows first-order kinetics, as expressed by eq. (7). When the curve-fitting procedure is applied to the data set after the contributions via eq. (7) have been eliminated by subtraction, however, elimination of sorbed molecules from the residual fraction ($\psi = < 0.1$) that is still in its rubbery state during the final sub-interval is seen to follow zero-order kinetics.

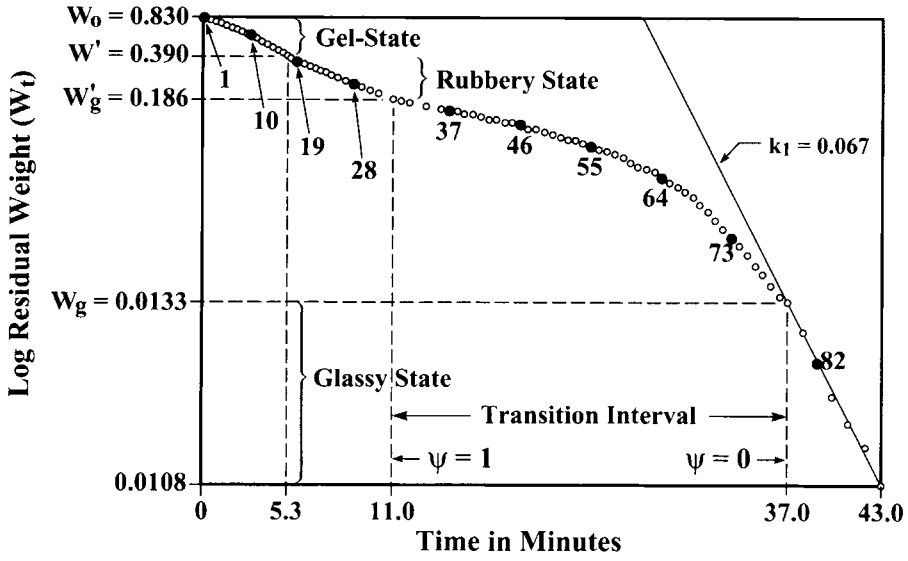

Figure 2A **Log W_t vs. t** plot for the methanol evaporation data (Fig. 1; pts. 1–80 in Table III). This plot shows the data after correction for contributions from the glassy state (Table III). The straight line through pts. 80–86 represents eq. (7) for the $i = 1$ population.

Extension of the computerized corrective operation fully back to the start of the transition interval, however, may be unnecessary because by definition the value of $1 - \psi$ at the start of the transition is virtually zero, and consequently correction during the initial part of the transition interval is negligible. Thus, the magnitude of error introduced by omitting correction through the first half of the transition interval is unimportant. This is confirmed by the small differences in the corresponding rate constants collected in Tables II and III because the correction is so much less than the contribution from the fraction ($\psi = > 0.7$) that is still in its rubbery state during the first half of the transition interval. It is concluded, therefore, that simple curve fitting to the original data set is usually sufficient to ascertain the kinetic order and the value of the corresponding rate constant for all the subintervals except those that

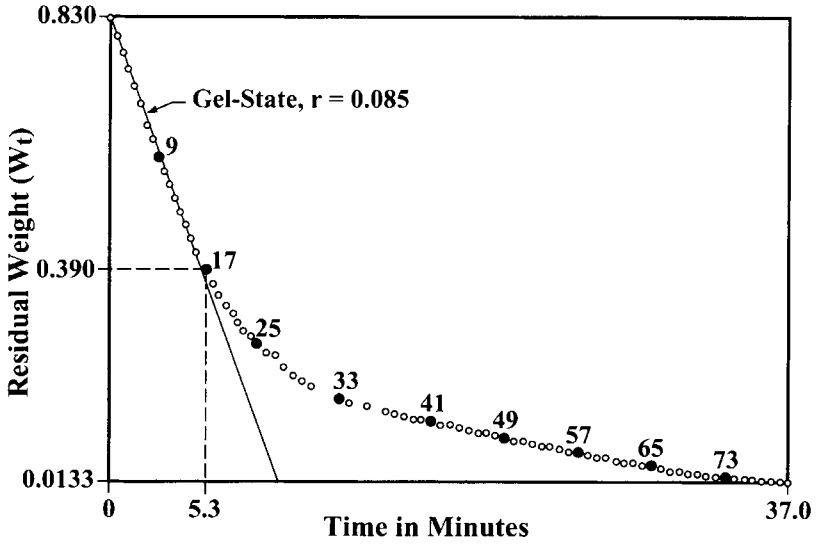

Figure 2B **W_t vs. t** plot for the methanol evaporation data (pts. 17–80 in Fig. 2A). The linear relationship [eq. (5)] identifies the interval required for elimination of the nonadsorbed molecules in the gel state from W_0 (pt. 1) to W' (pt. 17).

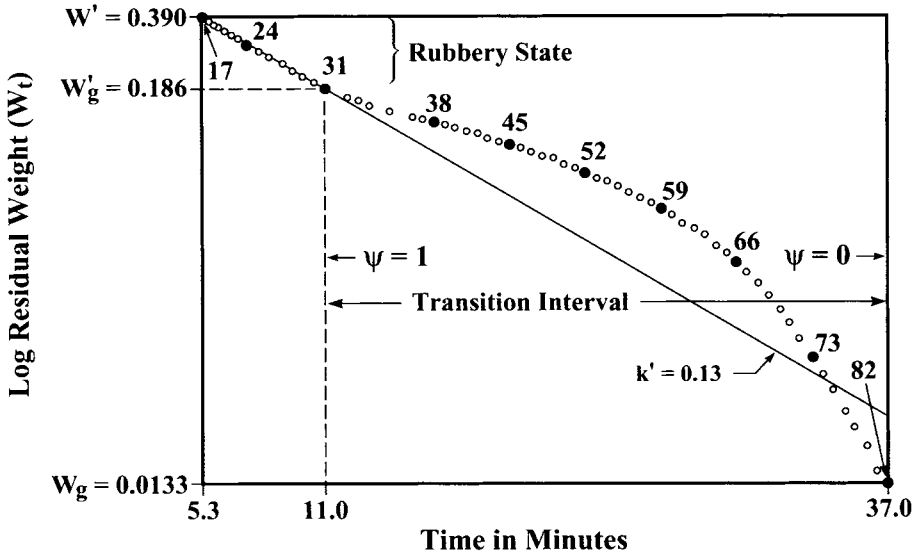

Figure 2C Log W_t vs. t plot for the methanol evaporation data (pts. 17–80 in Fig. 2B). The linear relationship [eq. (6)] identifies the interval for elimination of adsorbed molecules from the PS-L system in its rubbery state (pts. 17–31; $\psi = 1$) before the start of the transition interval at W'_g ($\psi = 1$; Table III).

occur at the very end of the transition intervals. Of course accurate characterization of these final subintervals would require that the original data set be corrected as described above. It is seen from the results collected in Tables II and III that none of the data points recorded during each of the four time studies of methanol evaporation are omitted in either curve-fitting procedure.

A typical example of curve-fitting to the data that had been so corrected is shown in the set of Figures 2A through 2F, which are computer-generated plots of the data for evaporation of sorbed methanol ("raw" data shown in Fig. 1) after point-by-point subtraction of the exponential decay functions [eq. (7)] for all but the population with the fastest decay rate in the glassy state. Subtraction of the contri-

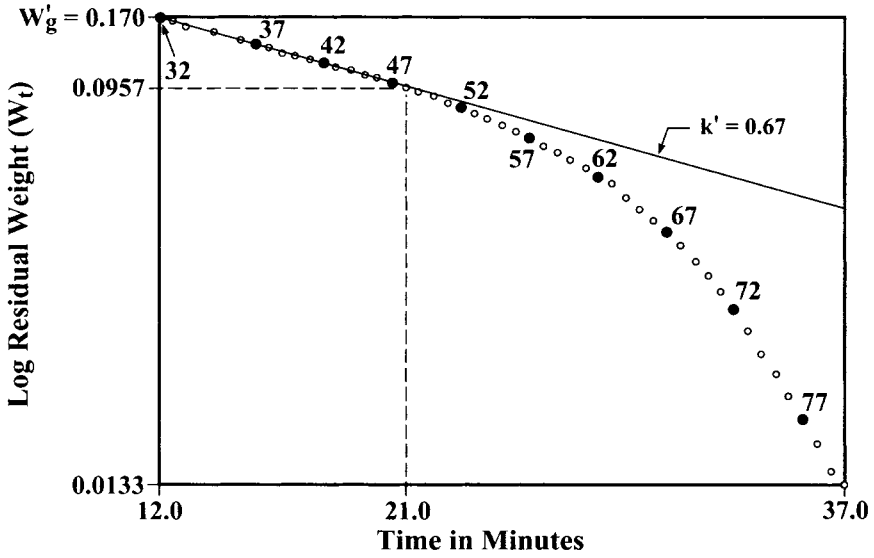

Figure 2D Log W_t vs. t plot for the methanol evaporation data (pts. 32–80 in Fig. 2C). The linear relationship [eq. (6)] identifies the first subinterval of first-order kinetics after the start of the transition interval at W'_g (pt. 32; $1 < \psi > 0.7$; Table III), and the subsequent deviation downward (pts. 49–80).

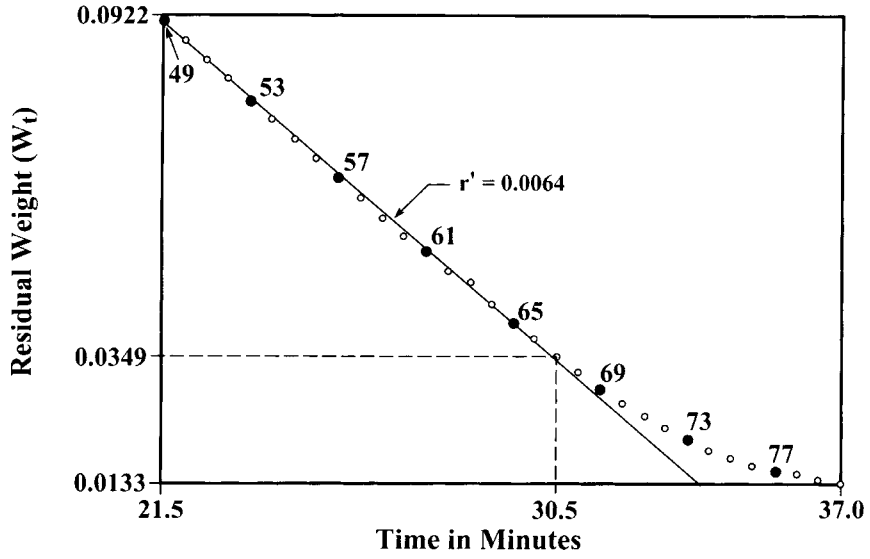

Figure 2E W_t **vs.** t plot for the methanol evaporation data (pts. 49–80 in Fig. 2D). The linear relationship [eq. (5)] identifies the first subinterval of zero-order kinetics (pts. 49–67) during the transition interval (pts. 32–80; $0.7 < \psi > 0.1$), and the subsequent deviation upward (pts. 67–80).

bution from population $i = 1$ was of course not performed because, as may be seen in Figure 2A, the result would be physically impossible.

Since the composition of the desorbed species in these time studies changes with W_t, as described earlier, ordinates of Figures 1 through 2F use W_t instead of α_t. The lines drawn from key points to the axes were added manually to provide convenient registry with the data recorded in Figure 1 and Tables II and III. Figure 2A is a Log W_t vs. t plot for points 1 to 86, showing the first-order straight line of best fit through data points 80 to 86, which represent the kinetics of decay for the $i = 1$ population trapped in the glassy state (i.e., the population with

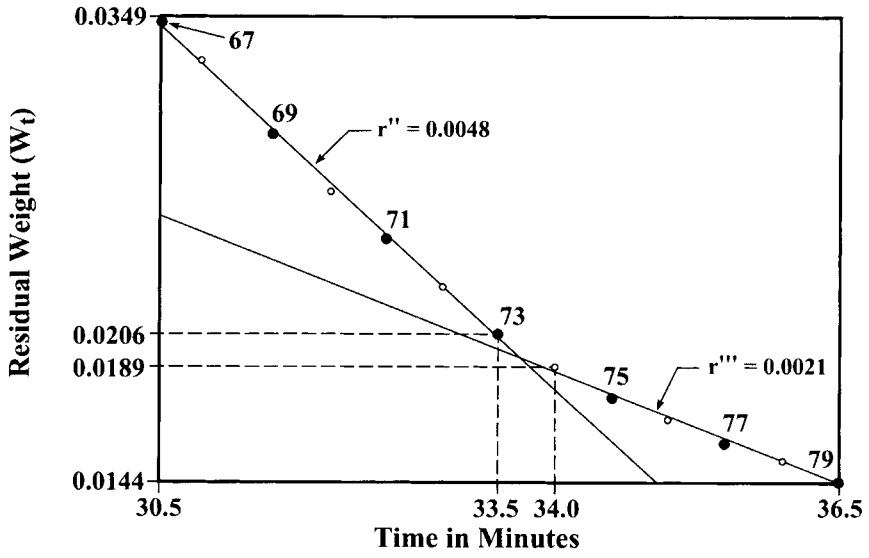

Figure 2F W_t **vs.** t plot for the methanol evaporation data (pts. 67–80 in Fig. 2E). The linear relationships [eq. (5)] identify the second (pts. 67–73) and third (pts. 74–79) subinterval of zero-order kinetics following after the first (pts. 49–67; Fig. 2E) during the transition interval (pts. 32–80; $\psi > 0.1$; Fig. 2D).

the fastest decay rate, isolated by sequential subtraction of the contributions from the populations with $i > 1$. The junction of this first-order straight line with the curved line at $t = 37$ minutes identifies the point that marks completion of transition from the rubbery state [i.e., when α_t becomes equal to α_g [eq. (10)]. The manner in which curve fitting was applied to the data points (1 to 80) taken before the PS–L system attained complete conversion to the glassy state is shown in Figure 2B to F. Figure 2B shows the straight line of best fit through points 1 to 16, which identifies the interval of zero-order kinetics [eq. (5)] for elimination of the sorbed-but-not-adsorbed molecules from the PS–L system in its gel state. The negative deviation (i.e., deviation upward) from the linearity of zero-order kinetics beginning at point 17 ($t = 5.3$ min) signals the composition that marks incipient elimination of adsorbed molecules [eq. (6)] from the PS–L system in its rubbery state; this follows first-order kinetics from pts. 17 to 31, as shown in Figure 2C. The sharp decrease in the first-order rate constant at point 31 marks the composition (W'_g; α'_g) that represents incipient transition from the rubbery state to the glassy state, as a result of evaporation-induced polymer–polymer association via one of (at least) two pathways. Figure 2D shows first-order kinetics for the data-points (32 to 48) that comprise the first subinterval of the transition interval, but with a rate-constant significantly less than that of the preceding interval (pts. 17 to 31; Fig. 2C). Positive deviation (i.e., deviation downward) from the linearity of first-order kinetics occurs at point 48 (Fig. 2D). This marks the start of a long interval over which the instantaneous rate of change in Log W_t is increasing. Figure 2E shows zero-order kinetics of evaporation during this subinterval (pts. 49 to 67), and upward deviation from the linearity expressed by eq 5 occurring eventually at pt. 68. The test for conformity to zero-order kinetics of the remaining data points (69 to 79; Fig. 2F) showed that this set spanned two successive sub-intervals of zero-order kinetics (i.e., from pts. 67 to 73 and from pts. 74 to 80) before the system attained the rigidity of the glassy state at pt. 80, as noted earlier in Figure 2A.

The results (Fig. 1 and Table I) observed in the first part of this study, which correlated the composition of desorbed molecules with the residual weight of the adsorbed molecules as the PS–L system was undergoing evaporation-induced transition from its rubbery ($\psi = 1$) to its glassy state ($\psi = 0$), showed that the abnormal kinetics exhibited during the second half of the transition interval was caused by an alternative pathway for this transition, and that this pathway involved concomitant expulsion of the adsorbed molecules. The results obtained in this, the second part of our restudy (Tables II and III, and Fig. 2A to F), show zero-order kinetics for this alternative pathway, which means that once this form of polymer–polymer association is initiated, it propagates at a virtually constant rate. It was also observed (Fig. 2E and F) that the zero-order rate constant for this pathway can decrease abruptly before the system attains the rigidity of a glassy state, presumably owing to a "catastrophic" readjustment of the molecular macrostructure in response to internal stresses that accumulate as the system evaporates toward the composition of a glassy state.

We now suggest that the mechanism for this alternative pathway involves a "domino"-like chain reaction, whereby (for example) two monomer units, on separate "solvated" polymer segments adjacent to a microdomain of self-associated polymer, are induced (thermodynamically) to undergo association, with concomitant expulsion of their adsorbed molecules, and that this in turn induces the next adjacent monomer units to undergo the same action. In this way polymer–polymer association via this chain reaction propagates at a constant rate, characteristic of the PS–L system, until the system attains the rigidity of a glassy state, after which W_t is given by eq. (7). Conceptually, the above model is a three-dimensional "zippering-up" of adjacent polymer segments to afford the corresponding three-dimensional network of associated polymer, containing residual trapped "guest" molecules which appear to be located in no more than six different molecular environments.

The above model implies that the molecules being eliminated from the PS–L system during the transition interval are derived concurrently from three different sources, which dominate the kinetics of elimination sequentially as the fraction (ψ) of the PS–L system that is still in its rubbery state decreases monotonically from 1 at the start of the transition to 0 at the end of the transition. Thus, when ψ is > 0.7, the kinetics is first order owing primarily to evaporation from the PS–L system still in its rubbery state; when ψ is < 0.7 but > 0.1, the kinetics become zero order owing to the expulsion of adsorbed molecules via the "zippering-up" mechanism; and when ψ is < 0.1, during the last stages of the transition interval, the contributions to the kinetics from the above two sources approaches zero, and consequently by default the kinetics is dominated by the molecules escaping from the fraction ($1 - \psi$) of the PS–L now in its glassy state, as expressed by eq. (7).

The "break-points" in the kinetics, which mark the start of the transition interval and subsequently the start of the subinterval(s) of zero-order kinetics, can be rationalized on the basis of progressive decrease in entropy and mobility of the solvated polymer segments as the PS–L system evaporates to dryness. When the change in free energy (i.e., $\Delta F = \Delta H - T\Delta S$) for undergoing polymer–polymer association with concomitant expulsion of the adsorbed molecules [eq. (13)] becomes less than zero, i.e., when the positive contribution of the product of temperature and change in entropy ($-T\Delta S$) no longer exceeds the negative contribution of the change in enthalpy (ΔH), association can occur as shown in eq. (13).

$$2P \cdot M_m \rightarrow P \cdot P + (2m)M \quad (13)$$

$$(2m)M + 2P - M_m \rightarrow 2P \cdot M_{2m} \quad (14)$$

Here P represents a polymer unit, M represents a volatile molecule, and m is the average number of adsorbed molecules M per unit P.

The probability that association will occur between two monomer units of different "solvated" polymer segments is obviously greatest when these solvated monomer units are in intimate contact with one another. When such action occurs during the first part of the transition interval (i.e., when ψ is > 0.7 and the mobility of the residual "solvated" polymer segments is still relatively high), the expelled molecules are easily readsorbed by the adjacent $P \cdot M_m$ units to form the corresponding $P \cdot M_{2m}$ units, as noted in eq. (14). Because these adjacent units are becoming temporarily more solvated, the term ($-T\Delta S$) for the immediate molecular environment changes to become equal to or greater than ΔH, and consequently the associative action via eq. (13) comes to an abrupt halt. The rigidity of the PS–L system increases accordingly owing to this formation of microdomains of self-associated polymer that serve as pseudo-crosslinkages, distributed randomly throughout the bulk of the PS–L system. We believe that such spasms of autocatalyzed associative action, which occur during the first part of the transition interval, are responsible for the observed sharp decrease in first-order rate constant without a qualitative change in kinetic order.

As W_t continues to decrease in accordance with the equivalent form of eq. (6), the mobility of the segments between covalent and/or pseudo-crosslinkages decreases accordingly (owing to normal evaporation-induced association that goes on continuously during the transition interval), and the change in free energy (ΔF) for polymer association, as expressed by eq. (13), becomes quite negative, so that the probability for the monomer units adjacent to the microdomains of already-self-associated polymer to initiate self-association [via eq. (13)] becomes quite high, whereas the probability for recapturing the expelled molecules [via eq. (14)] becomes quite low, owing to decreased segment mobility. Presumably the "breakpoint" in the zero-order kinetics during the last stages of the transition interval is caused by a "cataclysmic" alteration of the macromolecular structure, owing to accumulation of internal stresses, which serves to tighten further the rigidity of the PS–L system as ψ approaches 0.

Transition Intervals for Acetone, Chloroform, and Toluene PS–L Systems

Having developed the above model for the molecular changes that occur during the transition of a PS–L system from its rubbery state to its glassy state, using only the kinetic data collected during evaporation from a poly(Sty-co-DVB) sample that had been swelled to saturation in toluene and then deswelled "to saturation" in methanol, it was now of interest to establish the limits of this model, using the test liquids that exhibited significantly less-abnormal transition patterns (in the order acetone > chloroform > toluene, as indicated in Figs. 5, 7, and 9 of ref. 15).

The results observed for computerized curve-fitting to these three sets of data-points [before and after corrections for the contributions derived from the glassy state, as expressed by eq. (7)] are recorded in Tables IV, V, and VI, respectively. The data refer to the α_t values rather than the corresponding W_t-value from which α_t was calculated, because in these time studies both the nonadsorbed molecules and subsequently the residual adsorbed molecules were of the same species. These results show that curve fitting to the original data (i.e., before corrections for contributions from populations $i > 1$ trapped in the glassy state) produces a set of sequential subintervals that are characterized only by first-order kinetics, the rate constants of which decrease monotonically in the sequence that they occur. The computerized curve-fitting program, applied after the original sets of data points had been computer-corrected as above, not only corrects for the contribution from the fraction $(1 - \psi)$ of the PS–L system converted to the glassy state, but also identifies the data point where ψ is zero. The results obtained

Table IV Analysis of Data for Acetone Evaporation During the Transition Interval

Sample[a] State	Kinetic[b] Order	Rate[c] Constant	Data Points[d] P_i to P_f	Time Intervals[e] t_i to t_f	Composition[f] α_i to α_f	$R^{2\,g}$
(*Before* data "corrections" due to vitrification)						
Gel	0	(0.563)	1–8	0.0–3.5	3.13–1.03	0.9978
Rubbery	1	0.468	8–12	3.5–5.5	1.03–0.496	0.9935
Transition	1	0.0842	13–45	6.0–21.5	0.456–0.115	0.9993
	1	0.0640	45–48	21.5–23.5	0.115–0.105	0.9982
(*After* data "corrections" due to vitrification)						
Gel	0	(0.548)	1–8	0.0–3.5	3.13–1.03	0.9978
Rubbery	1	0.426	8–12	3.5–5.5	1.03–0.496	0.9939
Transition	1	0.120	13–30	6.0–14.5	0.496–0.219	0.9987
	0	(0.0156)	30–40	14.5–19.5	0.219–0.141	0.9978
	0	(0.0092)	41–46	19.5–22.5	0.135–0.111	0.9935
Glassy	1	0.230	46–69	22.5–37.0	0.111–0.072	0.9991
	1	0.0610	70–101	38.0–80.0	0.071–0.047	0.9993
	1	0.0100	102–115	87.0–337	0.045–0.020	0.9989
	1	0.0012*	116–118	420–1360	0.017–0.006	0.9999

Footnotes (a–e, and g) are the same as reported in footnotes (b–f, and h) in Table II. Footnote (f) reports α in adsorbed molecules per phenyl group of polymer (instead of W from which α is calculated).

The symbol * stresses that this value is the effective rate constant for a linear combination of three populations i = 3, 4, and 5 remaining at t = 1360 min, at which point the time study was terminated. The value of α_t at 1360 min was 0.0055, which represents 20% of the trapped acetone molecules that were present at t = 22.5 min, when α_t had attained a composition of the glassy state, i.e., α_g = 0.111.

Table V Analysis of Data for Chloroform Evaporation During the Transition Interval

Sample State[a]	Kinetic Order[b]	Rate Constant[c]	Data pts[d] P_i to P_f	Time Intervals[e] t_i to t_f	Composition[f] α_i to α_f	$R^{2\,g}$
(*Before* data "corrections" due to vitrification)						
Gel	0	(0.625)	1–12	0.0–5.5	6.127–2.678	0.9989
Rubbery	1	0.232	13–23	6.5–11.0	2.235–0.812	0.9989
Transition	1	0.126	23–26	11.0–12.5	0.812–0.671	0.9944
	1	0.060	27–51	13.0–30.0	0.641–0.228	0.9995
(*After* data "corrections" due to vitrification)						
Gel	0	(0.625)	1–12	0.0–5.5	6.127–2.678	0.9989
Rubbery	1	0.269	13–23	6.5–11.0	2.235–0.812	0.9991
Transition	1	0.169	23–26	11.0–12.5	0.812–0.671	0.9957
	1	0.0989	26–42	12.5–21.0	0.738–0.386	0.9992
	0	(0.0193)	43–48	22.0–27.0	0.364–0.270	0.9973
Glassy	1	0.193	49–57	28.0–40.0	0.255–0.155	0.9936
	1	0.0667	59–62	50.0–75.0	0.133–0.115	0.9999
	1	0.0086	63–68	85.0–288	0.110–0.0775	0.9993
	1	$0.0_3$48	69–71	436–1462	0.0681–0.0439	0.9997
	1	$0.0_4$61	73–83	7296–30130[h]	0.0048–0.0013	0.9897

Footnotes (a) through (g) are the same as reported in Table IV.

[h] The value of α_t at t = 30130 min was 0.00131, which represents 0.5% of the trapped chloroform molecules that were present at t = 28.0 min, when α_t had attained the composition of a glassy state, i.e., α_g = 0.255.

Table VI. Analysis of Data for Toluene Evaporation During the Transition Interval

Sample State[a]	Kinetic Order[b]	Rate Constant[c]	Data pts[d] P_i to P_f	Time Intervals[e] t_i to t_f	Composition[f] α_i to α_f	$R^{2\,g}$
(Before data correction due to vitrification)						
Gel	0	(0.1143)	1–41	0.0–23.0	4.533–1.830	0.9992
Rubbery	1	0.0698	42–58	24.0–40.0	1.727–0.584	0.9992
Transition	1	0.0382	59–63	42.0–50.0	0.529–0.389	0.9973
	1	0.0255	63–66	50.0–65.0	0.389–0.296	0.9953
	1	0.0118	67–70	78.0–105.0	0.216–0.157	0.9985
	1	0.0066	71–73	120.0–146.0	0.1137–0.115	0.9964
(After data correction due to vitrification)						
Gel	0	(0.1152)	1–44	0.0–26.0	4.533–1.534	0.9980
Rubbery	1	0.0797	44–58	26.0–40.0	1.534–0.584	0.9994
Transition	1	0.0463	59–64	42.0–55.0	0.529–0.336	0.9963
	1	0.0278	65–70	60.0–105.0	0.296–0.157	0.9994
	0	(0.0012)	70–72	105.0–131.0	0.157–0.126	0.9936
Glassy	1	0.0503	73–77	146–196	0.115–0.096	0.9957
	1	0.0069	78–87	210–438	0.094–0.078	0.9912
	1	0.0_366	88–96	1352–1863	0.060–0.055	0.9990
	1	0.0_426	97–98	5690–5830[h]	0.0397–0.0395	1.000

Footnotes (a) through (g) are the same as reported in Table IV.

[h] The value of α_t at t = 5830 min was 0.0395, which represents 34% of the trapped toluene molecules that were present at t = 146 min, when α_t had attained the composition of a glassy state, i.e., α_g = 0.115.

thereby show a parallel set of subintervals that now indicate a change to zero-order kinetics as ψ approaches zero, which is similar to that noted in the studies of methanol desorption (Tables II and III, and Figs. 2 to 7). The data collected in Tables IV, V, and VI also show that the ratio of the weight of molecules eliminated during the subintervals of zero-order kinetics to the total weight of molecules (eliminated during the entire transition interval) increases in the order that the pattern for evaporation during the respective transition intervals deviate from normalcy, namely acetone > chloroform > toluene (Figs. 5, 7, and 9 of ref. 15).

The respective computer plots of Log α_t vs. t, after correction for contributions from the glassy state, are shown in Figures 3A, 4A, and 5A. The coordinate values (α_t and t), for important data points and the respective range over which first-order (k) or zero-order (r) kinetics is followed, were added manually to provide convenient registry with the corresponding data collected in Tables IV, V, and VI. The data recorded in the intervals that deviate downward from the linearity of first-order kinetics, as shown in Figures 3A, 4A, and 5A, are replotted in Figures 3B, 4B, and 5B to test the respective conformities to zero-order kinetics, i.e., α_t vs. t. In every case the square of the correlation coefficient (R^2) to the straight line of best fit through each set of data points was greater than 0.99. It was interesting to note in the case of acetone evaporation that the kinetic data collected near the end of the transition interval actually spanned two subintervals of zero-order kinetics, the rate constants of which differed by a factor of about 2.

The above results (Tables IV, V, and VI and Figs. 3A to 5B) show that the manner by which zero-order kinetics dominates over first-order kinetics during the respective transition intervals, in the cases of acetone, chloroform, or toluene, is qualitatively similar to those exhibited by the corresponding PS–L systems containing methanol (Tables I to III and Figs. 1 to 2F). Consequently, we conclude that the presence of such sequential changes during the transition interval is a general phenomenon for evaporation-induced conversion of PS–L systems from the rubbery state (ψ = 1) to a glassy state (ψ = 0), and that the actual kinetic pattern for such transitions reflects the sequential changes in kinetics and thermodynamics characteristic of the PS–L system as it progresses from the mobility of the rubbery state to the rigidity of a glassy state.

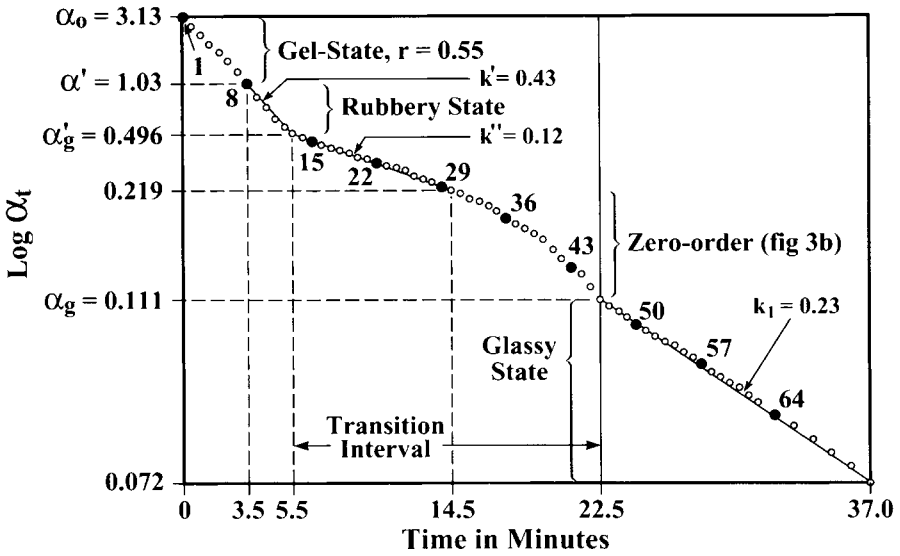

Figure 3A **Log α_t vs. t** plot for the acetone evaporation (pts. 1–69) after correcting for the contributions from the glassy state (Table IV). This plot identifies the rubbery state (pts. 8–14) before the start of the transition interval, the first subinterval of first-order kinetics (pts. 14–30) during the transition interval ($\psi > 0.5$), and the population ($i = 1$; pts. 46–69) with the fastest decay rate in the glassy state.

Thus, an "abnormal" pattern for a Log α_t vs t plot, which is markedly concave downward (as noted in the cases of methanol and acetone; Figs. 2A and 3A, respectively), indicates that the "normal" pathway for evaporation-induced polymer–polymer association which follows first-order kinetics, as expressed by eq. (6), becomes dominated early in the transition interval by the "abnormal" thermodynamically driven pathway of polymer–polymer association that causes expulsion of adsorbed molecules, and which follows zero-order kinetics. On the other hand, a pattern for the Log α_t vs t plot which

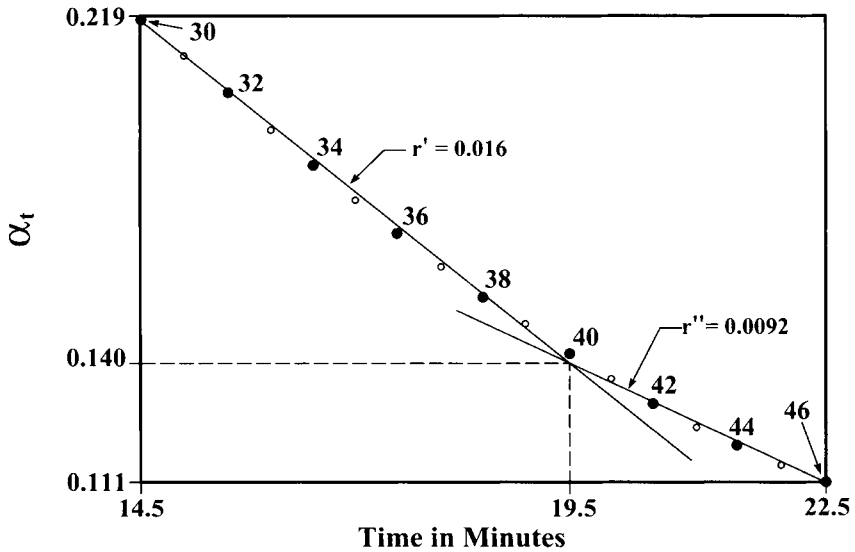

Figure 3B **α_t vs. t** plot for the acetone evaporation (pts. 30–46 of Fig. 3A). This plot identifies the first (pts. 30–40) and second (pts. 40–46) subintervals of zero-order kinetics during the transition interval ($\psi > 0.5$; Table IV and Fig. 3A).

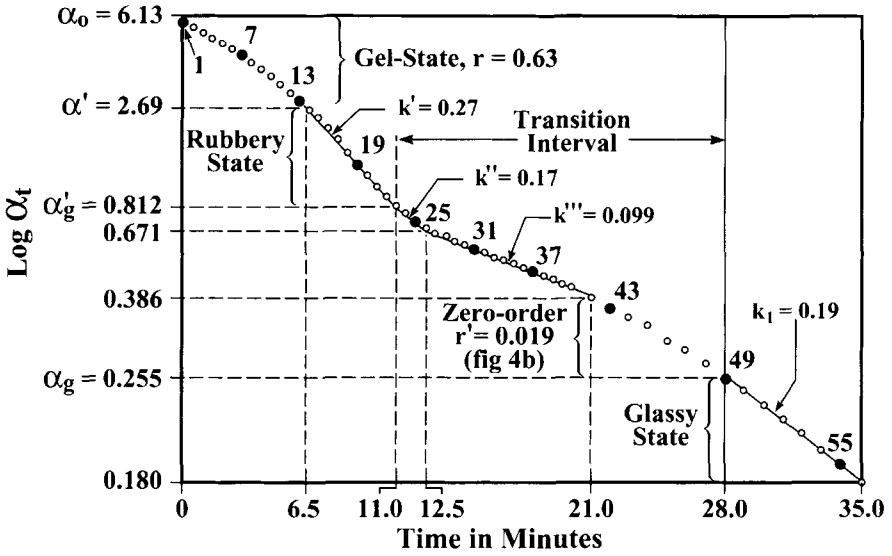

Figure 4A **Log α_t vs. t** plot for the chloroform evaporation (pts. 1–56) after correcting for the contributions from the glassy state (Table V). This plot identifies the rubbery state (pts. 14–23) before the start of the transition interval (pts. 23–49), the first (pts. 23–26) and second (pts. 26–42) subinterval of first-order kinetics during the transition interval ($\psi > 0.5$), and the population ($i = 1$; pts. 49–56) with the fastest decay rate in the glassy state, beginning at pt. 49.

is markedly concave upward (as noted in the case of toluene; Fig. 5A), usually indicates that the "normal" pathway does not become dominated by the "abnormal" one until the final stages of the transition interval.

Almost all of the transition patterns exhibited in our earlier time-studies of evaporation from PS–L systems that did not have a history of temporary exposure to a binary solution[7–15] were of the "normal" type, i.e., somewhere between those shown in

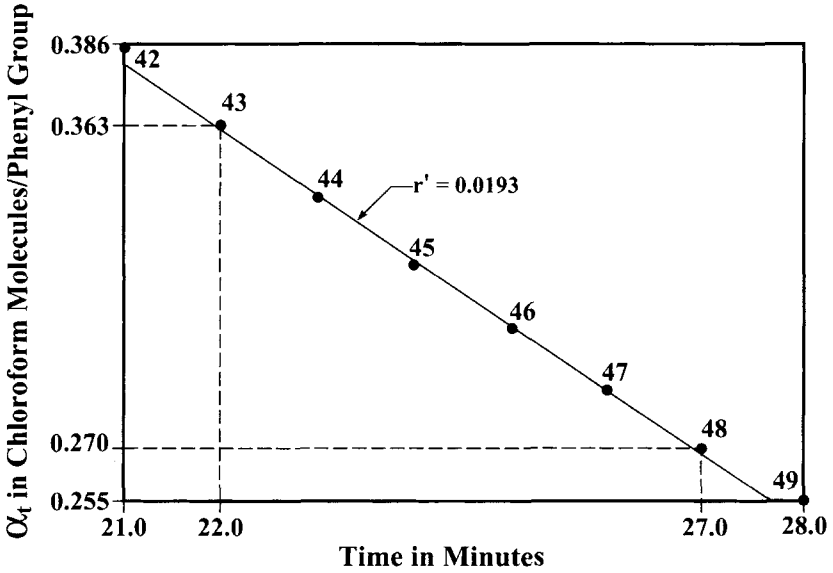

Figure 4B **α_t vs. t** plot for the chloroform evaporation (pts. 42–49 of Fig. 4A). This plot identifies the first (pts. 43–48) subinterval of zero-order kinetics during the transition interval ($\psi > 0.5$; Table V and Fig. 4A).

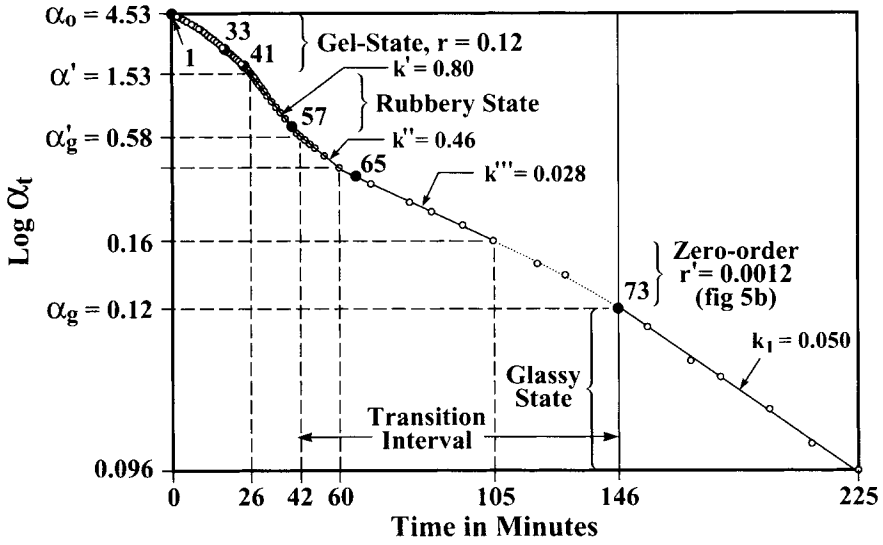

Figure 5A Log α_t vs. t plot for the toluene evaporation (pts. 1–79) after correcting for the contributions from the glassy state (Table VI). This plot identifies the rubbery state (pts. 44–58) before the start of the transition interval (pts. 59–73), the first (pts. 59–64) and second (pts. 65–70) subinterval of first-order kinetics during the transition interval ($\psi > 0.1$), and the population ($i = 1$; pts. 73–78) with the fastest decay rate in the glassy state, beginning at pt. 73.

Figures 7 and 9 of ref. 15 for chloroform and toluene, respectively. Application of computerized curve-fitting to the transition data collected in each of these time studies produced behavior falling between that reported here for chloroform and for toluene (Tables V and VI and Figs. 4A through 5B). In other words, computerized curve fitting to the original transition data produced only two or more long subintervals of first-order kinetics, the rate constants of which decreased with the sequence of their appearance; whereas the same procedure applied to the transition data set, after it was computer-corrected for contri-

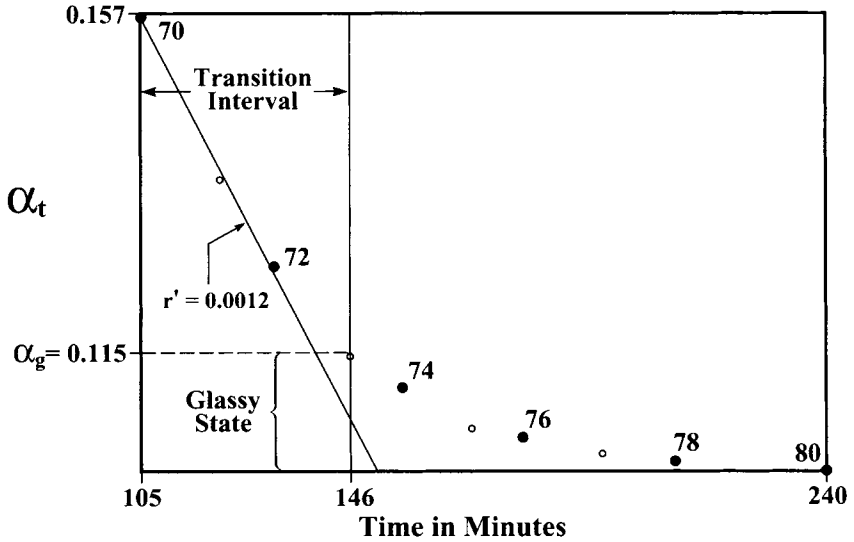

Figure 5B α_t vs. t plot for the toluene evaporation (pts. 70–80 of Fig. 5A). This plot identifies the sub-interval (pts. 70–72) of zero-order kinetics during the transition interval ($\psi > 0.5$; Table VI and Fig. 5A).

butions from the glassy state, produced two or more long subintervals of first-order kinetics followed at the very end of the transition interval by one or more short subintervals of zero-order kinetics, as noted here in Figure 5A and B. Only one marked exception was noted in this reconsideration of already published data. Surprisingly, this exception involved evaporation from a toluene-saturated PS–L system. The cause was not understood at the time, and it was attributed simply to "unknown factors" that affected the mode of transition from the rubbery state to the glassy state. The curve-fitting results observed for this exception, however, are consistent with those noted in the present studies for methanol (Tables II and III) and for acetone (Table IV). These results and the particular significance thereof will be reported in full at a later date.

Transition Interval for *n*-Heptane PS–L Systems

We stated in the preceding section that the manner in which a PS–L system undergoes evaporation-induced polymer–polymer association during the transition interval *usually* can be inferred qualitatively simply by visual inspection of the kinetic pattern exhibited during that interval. There are of course exceptions, which require full consideration via computerized curve fitting in order to arrive at a correct interpretation. Examples of such exceptions are found in the multireplicated time studies of *n*-heptane evaporation from PS–L liquid systems that had been swelled to saturation in toluene and then deswelled in *n*-heptane, and which are recorded in Figure 1 of ref. 15. These four time studies show that the patterns exhibited (after the breakpoint in the kinetics that signals completion of the interval required for elimination of the nonadsorbed molecules, and which follows zero-order kinetics), are very similar in form (albeit much shorter in time) to that noted for evaporation of toluene from such PS–L systems during the transition interval (Fig. 9 of ref. 15).

Application of computerized curve fitting to the original data verifies that the pattern of qualitative change in kinetic order over the intermediary subintervals of evaporation down to the glassy state in the case of *n*-heptane (Table VII) is quite similar to that noted for toluene evaporation (Table VI). The kinetics over the three or more intermediary subintervals [i.e., between the zero-order intervals required for elimination of the nonadsorbed molecules and the period for elimination of the residual molecules trapped in the glassy state (kinetically a linear combination of exponential decay functions)], all are first-order, the rate constants of which decrease monotonically in the sequence of their appearance. One might interpret this observation to mean that the manner in which the fraction (ψ) of the PS–L system still in its rubbery state undergoes transition to the glassy state is the same in both cases.

Table VII Analysis of Data for *n*-Heptane Evaporation During the Transition Interval (*Before* Data "Corrections" due to Vitrification)

Run[a]	State[b]	Order[c]	Rate Constant[d]	Data Points[e] P_i to P_f	Time[f] t_i to t_f	Composition[g] α_i to α_f	$R^{2\,h}$
1	Excess	0	(0.1613)	1–30	0.0–7.3	1.468–0.284	0.9982
	Trans.	1	0.4469	30–34	7.3–8.3	0.284–0.184	0.9897
		1	0.2842	34–38	8.3–9.3	0.185–0.140	0.9985
2	Excess	0	(0.1535)	1–16	0.0–5.0	1.001–0.241	0.9989
	Trans.	1	0.3913	16–18	5.0–5.7	0.241–0.186	0.9997
		1	0.2303	19–22	6.0–7.0	0.168–0.132	0.9889
		1	0.1208	23–25	7.3–8.3	0.125–0.116	0.9964
3	Excess	0	(0.2146)	1–14	0.0–3.3	0.980–0.267	0.9974
	Trans.	1	0.6316	14–17	3.3–4.0	0.267–0.168	0.9904
		1	0.3883	17–19	4.0–4.5	0.168–0.139	0.9729
4	Excess	0	(0.1841)	1–13	0.0–2.8	0.742–0.221	0.9992
	Trans.	1	0.4919	13–15	2.8–3.3	0.221–0.177	0.9989
		1	0.1656	16–18	4.0–5.0	0.150–0.127	0.9970
		1	0.0984	19–22	5.3–6.0	0.124–0.115	0.9915

Footnotes (a) through (g) are the same as reported in Table IV.

Excess in footnote (b) indicates that most of the non-adsorbed liquid is present as excess liquid sorbed in the interstices of the composite film sample before the start of the time study.

Such an interpretation, however, is not correct because it fails to take into consideration the history of the two PS–L systems before the start of the respective time studies of evaporations-to-dryness. In the case of toluene, all of the polymer component, after elimination of the nonadsorbed molecules from that PS–L system, was still in its rubbery state, i.e., ψ was equal to 1. In the case of *n*-heptane, however, more than 90% of the PS–L system had already undergone liquid-induced conversion to its glassy state even before the start of the time study, which means that the entire kinetics for evaporation-induced transition of the residual fraction ($\psi = < 0.2$) to its glassy state in the case of *n*-heptane corresponds to the last stages of that in the case of toluene. We noted in the preceding section, which discusses evaporation from systems not complicated by liquid-induced conversion to the glassy state before the start of the time study, that when ψ decreases to less than 0.1, the kinetics of evaporation is affected significantly by glassy-state contributions, i.e., $(1 - \psi) = > 0.8$. This means that in the case of *n*-heptane evaporation it is not possible to deduce the true pathway by which the residual polymer fraction ($\psi = < 0.2$) underwent evaporation-induced transition to the glassy state, unless the kinetic data collected after the interval of zero-order kinetics is corrected for contributions from the glassy major fraction $[(1 - \psi) = > 0.8]$, as described in the preceding section.

The data collected in the four time studies of *n*-heptane evaporation are recorded in Figure 1 of ref. 15 as α_t instead of as the corresponding W_t from which it was calculated, despite that almost all of the nonadsorbed molecules were *n*-heptane while the residual adsorbed material was a bicomponent mixture that contained as much as 50% toluene. Because the difference in the formula weights of the two components was relatively small, and the total weight of these residual trapped molecules represented only a very small fraction of the total weight of sorbed liquid at the start of the time studies, the error (introduced in the desorption pattern by the simplifying assumption that the absorbate is pure *n*-heptane) is very small.

Typical examples of computer plots of Log α_t vs. t and of α_t vs. t, after correction by subtraction of the contributions from populations $i > 1$ trapped in the glassy state, are shown in Figure 6A and B, respectively, and again in Figure 7A and B, respectively. The straight lines of best fit through the data points that comprise population $i = 1$ are shown in Figures 6A and 7A, and identify the data points that mark the composition (α_g) at the start of the glassy states in these two PS–L systems. The indications of α_t and t for these and other important data points were added manually to provide convenient registry with the data collected in Tables VII and VIII for all four time studies of *n*-heptane evaporation.

The curve-fitting values from point 1 to the data point that marks the composition α_g, which signals the completion of that transition interval, are collected in Table VIII. These results show that in every case the kinetics of the subintervals that comprise the transition intervals are zero order, not first order as noted in Table VII. These results confirm that most of the PS–L system that had undergone *n*-heptane-induced polymer–polymer association underwent subsequent conversion to the glassy state in the presence of excess binary solution, and that the mode in which the residual fraction ($\psi = < 0.1$) of the PS–L system, still in its rubbery state, underwent evaporation-induced transition to the glassy state, occurred *via* the "zippering-up" mechanism with concomitant expulsion of adsorbed molecules, the kinetics of which follow zero-order.

The Influence of History on the Macrostructure of the Glassy State

The results reported in previous publications[14,15] showed that the history of the PS–L system at liquid saturation can affect both its sorption capacity in a given solvent,[14] and subsequently the kinetics of evaporation of that system from saturation to dryness.[15] We noted that such history effects are manifested in the constants f_i and k_i of eq. (7), and k_0 and m of eq. (12), which quantify the elimination of residual molecules trapped in the PS–L system when it attains its glassy state.

Simple visual inspection of the ill-defined pattern of change in the kinetics of evaporation during the transition interval verified that history also affects the pattern of evaporation-induced transition from the rubbery state ($\psi = 1$) to the glassy state ($\psi = 0$). No attempt was made, however, to correlate these patterns with the decrease of ψ from 1 to 0, because it had been believed erroneously that ψ during this interval was a continuous function of time.

The results reported in the present publication show that during the transition interval the kinetics of evaporation change abruptly in a sequential manner that reflects the history of the PS–L system at liquid saturation. In general the kinetics of evaporation during the subintervals that comprise the earlier portions of the transition intervals is first order, the rate constants of which usually are in decreasing order; and the kinetics of evaporation dur-

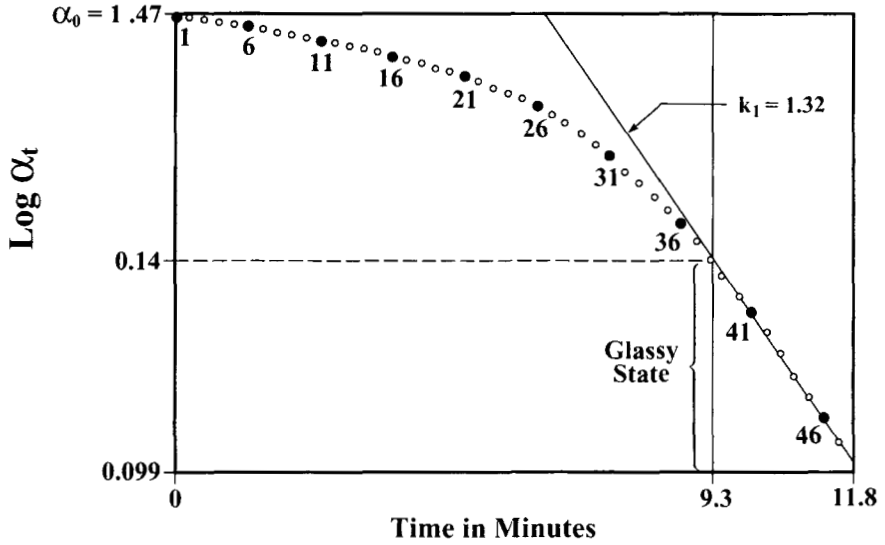

Figure 6A Log α_t vs. t plot for the n-heptane evaporation (Run No. 1 in Fig. 1 of ref. 15; pts. 1–48) after correcting for the contributions from the glassy state (Table VIII). The straight line through pts. 38–48 [eq. (7_1)] identifies the population ($i = 1$) with fastest decay rate in the glassy state.

ing the subintervals that comprise the later portions of the transition intervals is zero order, the rate constants of which also are in decreasing order. We postulate that a change in kinetic order or a sharp change in kinetic rate constant without change in kinetic order result from catastrophic changes in the polymolecular architecture of the PS–L system (owing to continued evaporation) that occur spasmodically to relieve accumulating stresses, and which increase accordingly the rigidity of the system. Thus, careful examination of the sequential changes in kinetic order that are exhibited after the interval

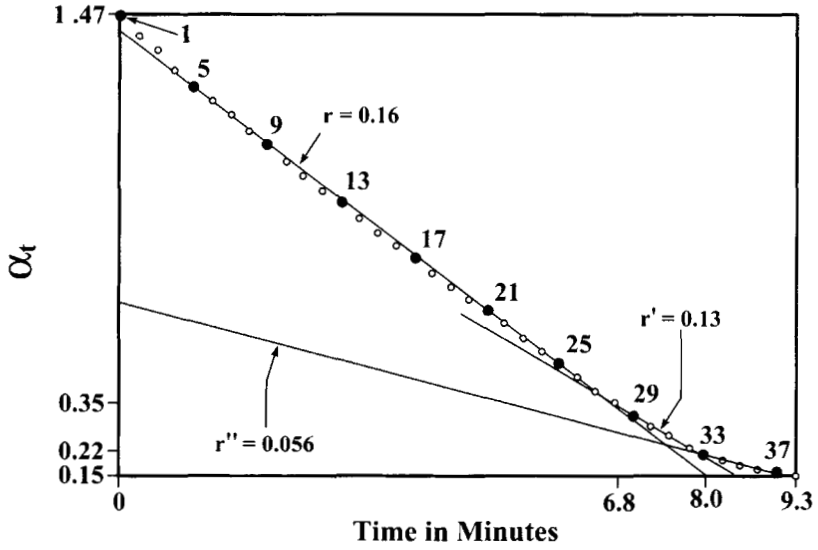

Figure 6B α_t vs. t plot for the n-heptane evaporation (pts. 70–80 of Fig. 5A). This plot identifies the interval of zero-order kinetics for elimination of the nonadsorbed molecules (pts. 1–28), and the two subintervals (pts. 28–33 and pts. 33–38) of zero-order kinetics that comprise the interval of evaporation induced transition (from $\psi < 0.2$ to $\psi = 0$; Table VIII and Fig. 6A) to the glassy state, beginning at pt. 38.

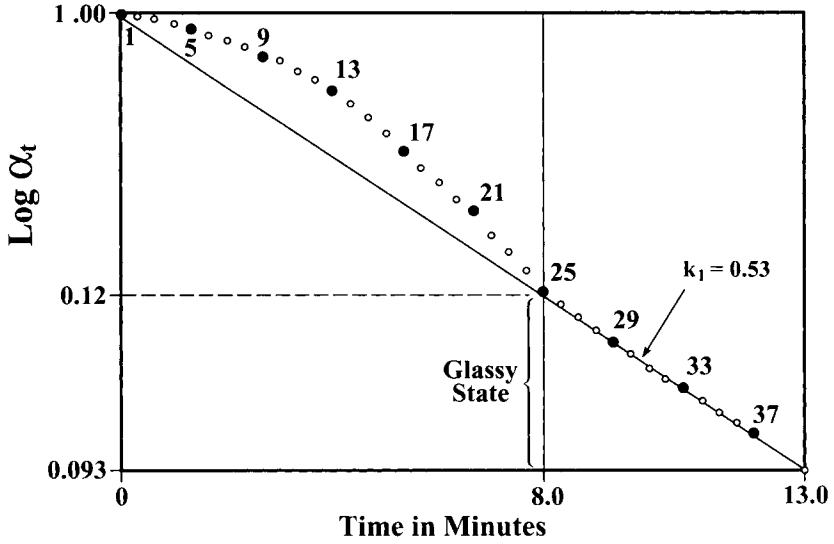

Figure 7A **Log α_t vs. t** plot for the n-heptane evaporation (Run No. 2 in Fig. 1 of ref. 15; pts. 1–38) after correcting for the contributions from the glassy state (Table VIII). The straight line through pts. 25–38 [eq. (7_1)] identifies the population ($i = 1$) with fastest decay rate in the glassy state.

required for elimination of adsorbed molecules allows one to infer the macrostructural state of the PS–L system (generated via liquid-induced polymer–polymer association) prior to the start of the time studies, as described above in the cases of methanol and n-heptane.

Although it is reasonable to expect that the interplay of the dual mechanism for elimination of residual adsorbed molecules during the transition interval should affect the constants that quantify the relationships [eqs. (7) and (11)] for subsequent elimination of residual molecules from the PS–L

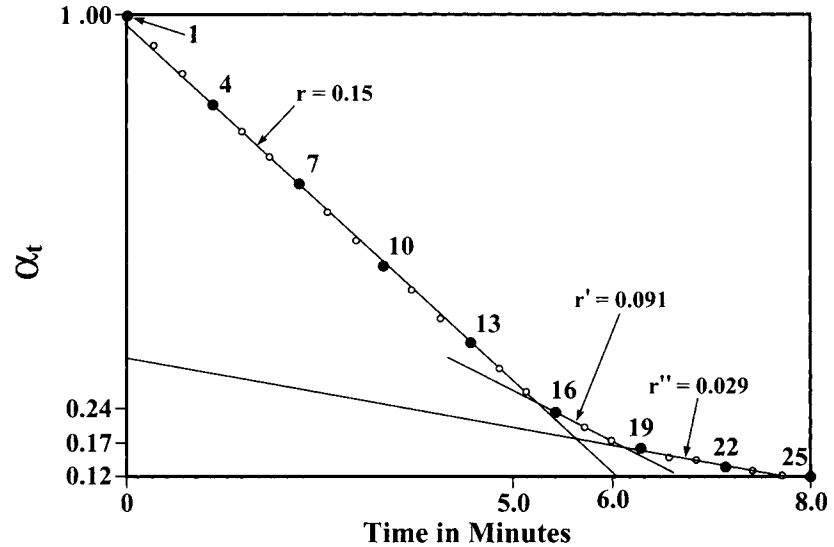

Figure 7B **α_t vs. t** plot for the n-heptane evaporation (pts. 1–25 of Fig. 7A). This plot identifies the interval of zero-order kinetics for elimination of the nonadsorbed molecules (pts. 1–16), and the two subintervals (pts. 16–18 and pts. 19–24) of zero-order kinetics that comprise the interval of evaporation induced transition (from $\psi < 0.2$ to $\psi = 0$; Table VIII) to the glassy state, beginning at pt. 25.

Table VIII Analysis of Data for *n*-Heptane Evaporation During the Transition Interval (*After* Data "Corrections" due to Vitrification)

Run[a]	State[b]	Order[c]	Rate Constant[d]	Data Points[d] P_i to P_f	Time[e] t_i to t_f	Composition[f] α_i to α_f	$R^{2\,g}$
1	Excess	0	(0.1628)	1–28	0.0–6.8	1.468–0.353	0.9983
	Trans.	0	(0.1295)	28–32	6.8–7.8	0.353–0.221	0.9984
		0	(0.0553)	33–37	8.0–9.0	0.205–0.149	0.9856
	Glassy	1	1.321	38–48	9.3–11.8	0.140–0.0994	0.9950
		1	0.2416	49–62	12.0–22.0	0.0981–0.0782	0.9992
		1	0.0388	63–73	25.0–92.0	0.0759–0.0616	0.9950
		1	0.00360	74–80	110–296	0.0601–0.0529	0.9944
		1	0.0_4961	81–85	345–1500	0.0518–0.0411	0.9820
2	Excess	0	(0.1535)	1–16	0.0–5.0	1.001–0.241	0.9995
	Trans.	0	(0.0911)	16–18	5.0–5.7	0.241–0.186	0.9931
		0	(0.0285)	19–24	6.0–7.7	0.168–0.120	0.9765
	Glassy	1	0.5329	25–38	8.0–13.0	0.116–0.0933	0.9982
		1	0.1331	39–51	14.0–30.0	0.0915–0.0784	0.9949
		1	0.0293	52–57	40.0–110	0.0749–0.0659	0.9938
		1	0.0_3593	58–61	200–252	0.0617–0.0599	1.000
3	Excess	0	(0.2149)	1–15	0.0–3.5	0.980–0.228	0.9971
	Trans.	0	(0.0792)	16–18	3.8–4.3	0.188–0.148	1.000
	Glassy	1	0.5721	19–30	4.5–13.0	0.139–0.0817	0.9776
		1	0.0569	31–97	14.0–80.0	0.0810–0.0658	0.9959
		1	0.00946	98–134	81.0–397	0.0658–0.0545	0.9993
		1	0.0_3285	135–139	436–541	0.0536–0.0520	1.000
4	Excess	0	(0.1841)	1–13	0.0–2.8	0.742–0.221	0.9992
	Trans.	0	(0.0974)	13–15	2.8–3.3	0.221–0.177	0.9959
		0	(0.0184)	16–21	4.0–5.8	0.150–0.177	0.9961
	Glassy	1	0.4924	22–39	6.0–10.5	0.115–0.0977	0.9989
		1	0.0841	40–66	11.0–45.0	0.0968–0.0788	0.9923
		1	0.0178	67–79	50.0–150	0.0791–0.0704	0.9836
		1	0.00240	80–91	180–540	0.0690–0.0608	0.9981
		1	0.0_4364	92–102	1551–8283	0.0537–0.0419	0.9949

Footnotes (a to h) are the same as reported in Table VII.

system in its glassy state, it was not possible to establish a good cause-and-effect relationship. Apparently there are other factors, not yet identified, that affect population distribution in the glassy state, and as a result the physical properties of the dried product. Obviously, this newly identified area of polymer technology will benefit from considerably more research.

Our reconsideration of the kinetics of evaporation during the transition interval improved our understanding of the molecular changes that occur during this interval. In addition it helped clarify a very puzzling observation that occurs on rare occasions after the PS–L system has attained the rigidity characteristic of the glassy state, namely that the plot of Log α_t vs. t exhibits an "abnormal" run of data, in which the rate of elimination of molecules trapped in the glassy state increase sharply but temporarily. This perturbation appeared to be relatively insignificant in the overall Log α_t vs. t plot. Nevertheless, when the contributions from each of the glassy-state populations that has been formed at the completion of the transition interval ($\alpha_t = \alpha_g$) were subtracted sequentially, as described above, the "abnormal" run of data was unmistakably significant. The relationships [eqs ($12_{,n}$) to ($12_{,1}$)] obtained thereby showed that the "abnormality" always occurred during the last portion of an interval required to eliminate a given population (usually i = 2, 3 or 4), and that the shape of such "perturbations" resembled the data patterns of the subintervals that represented the disappearance of the rubbery state, as noted in Figures 2A, 3A, 4A, and 5A, the kinetics of which was observed to follow zero-order. In view of this similarity, we decided to test the "abnormal" data set for conformity to zero-order kinetics. We ob-

served that in every case the square of the correlation coefficient (R^2) for such a linear relationship was always greater than 0.98. An example of such a "perturbation" is reported in Table III. It occurred in the second time-study for methanol desorption from poly(Sty-co-DVB) in the glassy state, between the $i = 1$ population (pts. 85 to 98) and the $i = 2$ population (pts. 104 to 107). Although the zero-order behavior suggests a common origin for both "abnormalities," the molecular nature of the phenomena that cause these two "perturbations" cannot be the same. One is caused by the thermodynamically driven polymer–polymer association converting rubber to glass with concomitant expulsion of residual adsorbed molecules, whereas the other is caused by cumulative internal stresses[16] in the glass owing to progressive elimination of trapped molecules. This internal stress exerts forces on the residual populations of polymer inclusion complexes via their polymer chains. Eventually, these internal stresses become strong enough to pull away the "host" polymer segments that serve to restrain the "guest" molecules still entrapped therein. In so doing the internal stress is relieved to the extent that the polymer chain was "disentangled." The "guest" molecules liberated thereby are now able to move "normally" through the bulk of the system at a rate much faster than the rate of escape from the confines of the former intact inclusion complex.

LIST OF SYMBOLS AND NOTATIONS

α The average number of adsorbed molecules per accessible phenyl group in the PS–L system at liquid-saturation [eqs. (3) and (4)]

α' The average number of residual adsorbed molecules per phenyl group after elimination of the nonadsorbed molecules from the PS–L system [eqs. (6) and (8)].

α'_g The average number of residual adsorbed molecules per phenyl group that marks incipient transition of the PS–L system from its rubbery to its glassy state [eq. (10)].

α_g The average number of residual adsorbed molecules per phenyl group that marks the completion of transition to the glassy state [eqs. (7) and (10)].

α_0 The average number of sorbed molecules per phenyl group at the start of a time study [eq. (5)].

α_t The average number of residual adsorbed molecules per phenyl group at time t after the start of a time study [eqs. (5), (6), and (7)].

α_i The average number of residual adsorbed molecules per phenyl group at the *start* of a specific interval of evaporation in a time study (Tables IV through VIII), or the portion of α_g that is in the i-th population, i.e., $\alpha_i = f_i\alpha_g$ [eq. (7)].

α_f The average number of residual adsorbed molecules per phenyl group at the *end* of a specific interval of evaporation in a time study (Tables IV through VIII).

[W, W', W'_g, W_g, W_0, W_t, W_i, W_f are the weights of absorbed molecules per gram of polymer, from which the above set of α-values were calculated].

C The relative swelling power of the sorbed liquid (in mL of adsorbed liquid) per gram of polymer [eqs. (1) to (3)].

χ The Flory-Huggins Interaction Parameter [eq. (2)].

χ_ν χ-value for a PS–L system the polymer volume fraction of which is ν [eq. (2)].

f_i The fraction of residual adsorbed molecules trapped in the i-th population of a PS–L system at the completion of the transition interval, i.e., $f_i = \alpha_i/\alpha_g$ [eq. (7)].

ϕ The toluene mole-fraction of molecules sorbed by a PS–L sample.

i Identification number of the population of molecules trapped in the glassy state in the order of decreasing decay rate [eqs. (7) and (11)].

k' First-order rate constant for evaporation from a PS–L system in its rubbery state [eq. (6)].

k_i First-order rate constant for decay of the ith population trapped in the glassy state [eq. (7)].

k_0 The k_i-value extrapolated to $i = 0$ [eq. (11)].

λ The average number of backbone carbon atoms in the polymer segments between crosslinked junctions in the poly(Sty-co-DVB) sample [eq. (1)].

λ_0 The value of λ extrapolated to $\mathbf{S} = \mathbf{0}$ [eq. (1)].

Λ The relative looseness of the polymeric architecture as given by the difference $(\lambda^{1/3} - \lambda_0^{1/3})$ [eqs. (1) and (4)].

m The decrementation constant for the incremental decrease in Log k_i [eq. (11)].

P Data point of a time study.

P_i Data point at the *start* of a given interval of a time study (Tables II to VIII).

P_f Data point at the *end* of a given interval of a time study (Tables II to VIII).

PS–L Polystyrene–liquid system.

r The zero-order rate constant in either grams of sorbed molecules per gram of polymer per minute, or the number of sorbed molecules per phenyl group per minute [eq. (5)].

S The volume (in mL) of sorbed liquid per gram of polymer at liquid saturation [eq. (1)].

Σ The total number of sorbed molecules, both adsorbed and nonadsorbed, per phenyl group of a PS–L system at liquid saturation [eq. (4)].

t Time in minutes after a given reference point in a time study.

t_i Time at the *start* of a given interval of a time study (Tables II to VIII).

t_f Time at the *end* of a given interval of a time study (Tables II to VIII).

τ Time that a PS–L system, which had been swelled first in toluene and deswelled in a test liquid, was extracted continuously in fresh test liquid before the start of the time study.

ψ The fraction of the polymer in a PS–L system that is still in its rubbery state.

$1 - \psi$ The fraction of the polymer in a PS–L system that has been converted to the glassy state.

z The volume fraction of toluene in the sorbed binary solution.

REFERENCES

1. L. A. Errede, in *Advances in Polymer Science,* T. Saegusa, Ed. Springer Verlag, Berlin-Heidelberg, 1991.
2. L. A. Errede, *J. Appl. Polym. Sci.,* **31,** 1749 (1986).
3. L. A. Errede, *J. Phys. Chem.,* (a) **93,** 2668 (1989); (b) **94,** 466 (1990); (c) **94,** 3851 (1990); (d) **94,** 4338 (1990); (e) **95,** 1836 (1991); (f) **96,** 3537 (1992).
4. L. A. Errede, *Polymer,* **33,** 2168 (1992).
5. L. A. Errede, *J. Appl. Pol. Sci.,* **45,** 619 (1992).
6. L. A. Errede, M. J. Kueker, G. V. D. Tiers, and J. W. C. Van Bogart, *J. Polym. Sci: Part A.: Polym. Chem. Ed.,* **27,** 2019 (1988).
7. L. A. Errede and J. W. C. Van Bogart, *J. Polym. Sci: Part A.: Polym. Chem. Ed.,* **27,** 2019 (1989).
8. L. A. Errede, *J. Polym. Sci: Part A.: Polym. Chem. Ed.,* **28,** 837 (1990).
9. L. A. Errede, *J. Polym. Sci: Part A.: Polym. Chem. Ed.,* **28,** 857 (1990).
10. L. A. Errede, G. V. D. Tiers, J. E. Trend, and B. B. Wright, *J. Polym. Sci: Part A.: Polym. Chem. Ed.,* **30,** 1129 (1992).
11. L. A. Errede, E. B. Aus, and R. W. Duerst, *J. Polym. Sci: Part A: Polym. Chem. Ed.,* **30,** 1145 (1992).
12. L. A. Errede and R. A. Newmark, *J. Polym. Sci: Part A: Polym. Chem. Ed.,* **30,** 1155 (1992).
13. L. A. Errede, P. J. Henrich, R. A. Pearson, and J. W. C. Van Bogart, *J. Polym. Sci: Part A: Polym. Chem. Ed.,* **31,** 805 (1993).
14. L. A. Errede and S. C. Hanson, *Polymer Swelling,* part 15 this journal.
15. L. A. Errede, P. J. Henrich, and J. N. Schroepfer, *J. Appl. Polym. Sci.,* **54,** 649 (1994).
16. S. G. Croll, *J. Coatings Technol.,* **51,** 64 (1979).

Received September 24, 1993
Accepted April 15, 1994